CODEN:LUTEDX/(TEIE-5310)/1-68/(2013)

Industrial Electrical Engineering and Automation

Inductive Energy Transfer

Vehicular Application

Alexander Svensson

Division of Industrial Electrical Engineering and Automation
Faculty of Engineering, Lund University

Abstract
With the diminishing reserves of oil and the growing public concern for environmental issues, the end of gasoline powered vehicles is getting closer each year. To prevent this from causing the personal and comfortable way of transportation mankind has gotten used to, to die with them, an alternative without the downsides of the gasoline engine must be developed. The environmentally friendly electric vehicle is such an alternative, but this comes with problems of its own, range and charging time.

A way to solve these problems is to charge the vehicles continuously from the road, which could be done through inductive power transfer. Such systems exist but because of large air gap they are large and impractical on a large scale. By combining this with air bearing it could enable the air gap to be greatly reduced, leading to less material and power requirements.

Through simulations and calculations regarding inductive power transfer, a model for transferring the necessary power was designed to show whether air bearing can be used with this technique to decrease the air gap and minimise the material and power needed.

The tests show that transferring the required power is feasible even when everything is scaled down as a result of a smaller air gap. From a receiver of roughly 200 mm times 100 mm, 30 kW can be delivered to the car's engine and battery, and for a lorry six of these receivers provide almost 200 kW.

Although there are still optimisations to be made, the results show that combining inductive power transfer with air bearing could be the solution for making continuous charging from the road possible in the future. With this, electric vehicles could make gasoline obsolete as fuel for personal transportation.

Prelude
This report is the result of a master thesis project done at Lund Institute of Technology (LTH), from January 2013 to June 2013.

As fort the people involved in this project, I would first of all like to thank Bryan Richards for coming up with the idea of combining air bearing with continuous inductive power transfer for vehicles, and for the illustrations he made for this report to really show how the different parts could look which helps with understanding the report. In addition I would like to thank Mats Alaküla for suggesting this as a master thesis and initiating it in the very beginning. Last but certainly not least, I would like to thank Avo Reinap, my supervisor at LTH, for the support, help and feedback he has provided during the course of this semester.

I would also like to mention the contributions made by my friends Niklas Berg and Samuel Estenlund, with whom I have been able to bounce ideas off of when the need arose.

Table of Contents

1 Introduction 1

1.1 Background 1

1.2 Objective 2

1.3 Structure of thesis 3

1.4 Method 3

2 Concept 3

2.1 Partially coupled transformer model 6

2.2 Design parameters 10

2.3 Complex power compensation 11

2.4 Hover techniques 13

2.4.1 Air bearing 13

2.4.2 Magnetic levitation 16

2.5 Shielding 16

2.6 Losses 17

2.6.1 Conductive losses 17

2.6.2 Core losses 19

2.6.3 Switching losses 21

2.7 Road side 22

3 Existing solutions 22

3.1 Stationary inductive power transfer 22

3.2 KAIST and OLEV Technology 22

3.3 PRIMOVE 23

4 Evaluation model 24

4.1 Specifications 24

4.2 Power transfer model 25

4.3 Power loss model 26

4.4 System model 27

5 Results 28

5.1 Power transfer capability 28

5.1.1 Conventional road solution 29

5.1.2 Ideal road solution 31

5.2 Power transfer efficiency 34

5.2.1 Conventional road solution 34

5.2.2 Ideal road solution 35
5.3 Scalability 38
5.3.1 Traditional road solution 38
5.3.2 Ideal road solution 38
5.4 Hovering 39
5.5 Shielding 40
6 Analysis 41
7 Design examples 43
7.1 Conventional road solution 44
7.2 Ideal road solution 45
8 Conclusion 45
9 References 47
10 Appendix 51
10.1 Classic electrodynamics 51
10.1.1 Maxwell's equations 51
10.1.2 Inductance and mutual inductance 54
10.1.3 Flux linkage of coils 55
10.1.4 Electromotive force 56
10.2 Power electronics 56
10.2.1 Frequency changer 56
10.2.2 Rectifier 57
10.2.3 Power inverter 60
10.2.4 Complex power 61
10.3 Three-phase transformer matrix 63
10.4 AC-resistance due to proximity effect 64

1 Introduction

1.1 Background

During the late 19th and early 20th century, the electric vehicles took up a significant part of the automobile market. Despite the drawbacks of low speed and long start-up times, these cars were still preferred because they did not suffer from vibration, smell and noise, whereas the cars with gasoline engines did. Another advantage over the competition was that there was no need for gear shifting; one of the most difficult task for the owners of the early gasoline powered cars. Although the range was a problem, the electric cars were primarily used in cities where the distances were short. However as the road infrastructure between cities was improved, the need for vehicles with longer range increased and thus electric vehicles began to be phased out and gasoline became the fuel of choice.

With the possibility for every person to make long trips individually and at their own time, the world of transportation changed into something never seen before. This luxury of personal and cheap transportation has even shaped much of the modern world, with how we live, work and shop. Today it is for most people impossible to imagine a life without the level of freedom the gasoline cars have provided. At the centre of this way of life, this technology, is oil; the substance from which gasoline, and therefore our way of living, is made.

Today it is known that the world's oil reserves are reducing and that sooner or later they will become commercially irrelevant. Exactly when the peak in production is going to, or did occur and when mankind will have to make do without it is widely discussed, but that a future without oil is imminent is a reality which cannot be ignored.

Another issue with the gasoline engine is the pollution it generates. In a world where environmental awareness is growing, the negative effect is just as an important problem for the gasoline engine as the decreasing oil reserves.

Faced with this future and the increasing gas prices coming with it, alternative solutions to make it possible to keep this life standard we are used to, is researched. Such alternatives include diesel, hybrid, biofuel and hydrogen engines. Problems regarding these are that diesel and hybrid vehicles still rely on oil to function, biofuel is controversial because food is used to produce the fuel, and hydrogen require much energy to produce.

Another possible solution to maintain our current level of comfort regarding personal transportation is dating back to electric vehicles. These run directly on electrical energy, so there are no pollutions being expelled while driving and they are much more efficient than traditional engines. Just like around the turn of the 20th century most trips made by car are within a city and are therefore relatively short. Electric vehicles are designed to make such trips with ease and if they can be recharged while parked, most people could transfer to an electric vehicle without any major downsides.

One major problem that does exists for electrical vehicles is the energy itself. If the energy production used to power the electric cars is based on fossil fuels, the environmental issues of the gasoline engine remains. If the increased need for energy in the world is met with more power being

generated by other fossil fuels, such as coal, the positive net result for the environment from not driving on gasoline anymore does not get any better. That is why it is important to, parallel with phasing out vehicles driving on gasoline; exchange the energy production to cleaner, more environmental friendly alternatives.

However electrical vehicles have technical problems too, problems that are crucial to solve if this is to become the solution that replaces oil and gasoline engines. The first problem is with regards to range, again just like it was over 100 years ago. For longer journeys a lot of energy is required which means that the vehicle needs large capacity for stored energy, i.e. many batteries. These are heavy, which decreases range because more energy is needed to propel the vehicle and also very expensive which makes it economically questionable. Another problem connected with capacity is charging.

To be able to drive long distances much energy is as previously stated needed, and when the batteries need to be recharged it takes a long time. Charging times up to 10 hours is nothing out of the ordinary and together with the limited range, makes longer journeys with electric vehicles impossible. A lot of work is done to speed up charging time and solutions for quick charging are many and techniques are developed to cut the time down to 1 hour, 30 minutes or lower. However it still shows that charging time is a problem and to get range equivalent to that of gasoline engines, many batteries are needed even if charging time is reduced to the same as refuelling a car.

A completely different approach to these problems is continuous charging while driving. The idea is to do so during long drives where the vehicle's batteries are not enough. For trips around town the batteries' capacity is enough and in combination with charging while the vehicle is parked, range and charging time is never going to be a problem. This can be done in three different ways; conductive, inductive or capacitive power transfer.

1.2 Objective

As stated in the background, there are three methods to transfer electrical energy; the conductive, inductive and capacitive method. In this master thesis it is the inductive method that is studied. More specifically is that it is studied as a method to power and charge electric vehicles continuously while driving. Two different levels of power is set; 30 kW for cars (20 for propulsion and 10 kW for charging the batteries), and 200 kW for lorries (150 for propulsion and 50 kW for charging the batteries). The main objective is to study how a large magnetic air gap and a high power can be compromised for best performance. It is also combined with air bearing as a method to minimize the air gap between the two transformer halves, thus also the size of and cost for them, an idea proposed by Mr Bryan Richards at Boeing (US patent pending, Bryan B. Richards, "Electrical connection device for electric vehicles"). Some general thoughts and ideas regarding the system behind the power transfer is also be discussed, but these are not a part of the simulations or calculations. An illustration of the concept is shown in Figure 1.

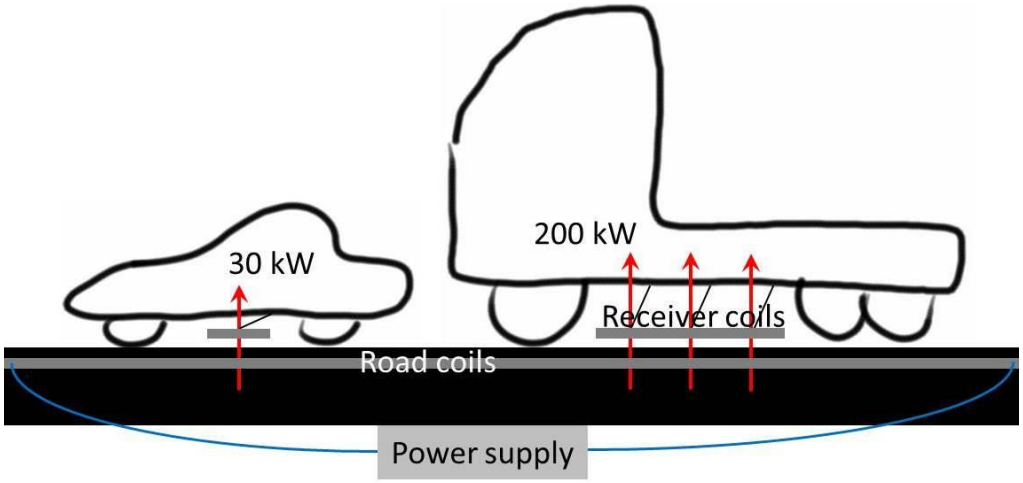

Figure 1: Sketch showing the conceptual idea for this thesis.

1.3 Structure of thesis

The structure of this report is the following:

After the introduction, chapter two focuses on the concept behind the technique to transfer power wirelessly and problems surrounding it, and air bearing.

Chapter three focuses on existing solutions for wireless power transfer, while chapter four describes the solution proposed in this report.

The results from the work done is presented in chapter five, and analysed in chapter six.

The detailed description of this solution is found in chapter seven with the final conclusions in chapter eight.

Chapters nine and ten is the reference list and the appendix, the latter containing descriptions of the basic physics behind magnetic fields, wireless power transfer and power electronics.

1.4 Method

All simulations regarding the magnetic problems of this thesis are made in the free 2D software *Finite Element Method Magnetics* (FEMM), owned by David Meeker, Ph.D. Available from: www.femm.info. These simulations are done statically since the magnetic coupling and leakage inductance are the main input for the simulation model.

The data interpretation and all calculations are made in *Matlab*, by The MatWorks, Inc. Namely the simulation model based on equivalent circuit in which the operation points and frequency sweeps are analysed.

2 Concept

To achieve the inductive power transfer, coils in a three-phase configuration are placed in the road along its length and all cars are equipped with one three-phase section of the same configuration as in the road. The part in the car is then lowered from the chassis by an arm, and with air bearing it hovers at a determined height to minimise the air gap (see Figure 2 and), and therefore also the size of the coils and core, the power required and the cost.

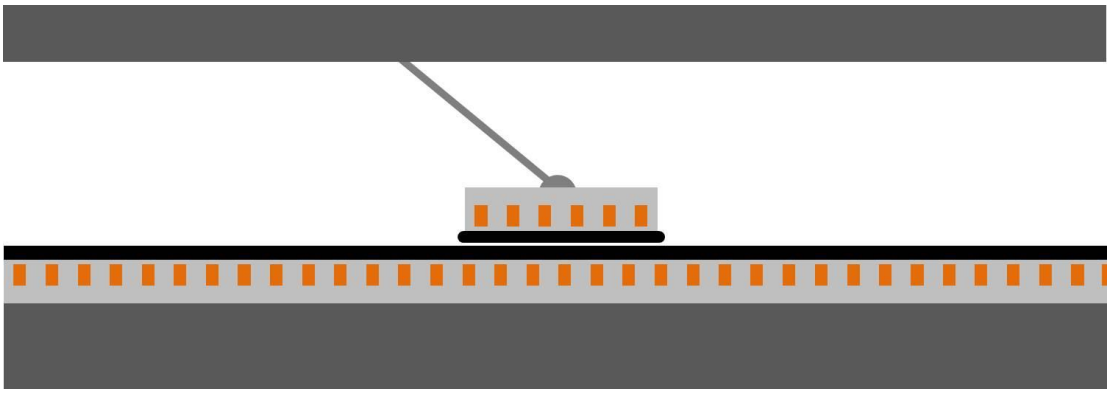

Figure 2: Cross sectional view of the system seen from the side.

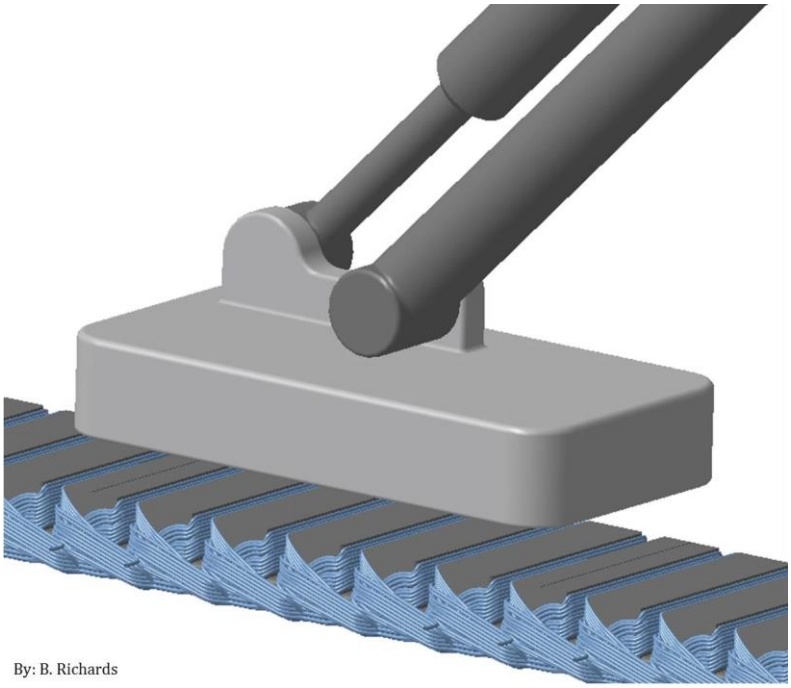

Figure 3: 3D view of the system with the road side part uncovered.

The basic concept of how the inductive power transfer is done is by imagining a regular three-phase electric motor cut open and unfolded, as illustrated in Figure 4. Both machine layouts show that overlapping windings are used, and the advantage of this is that it leads to a higher coupling factor due to larger areas of the coils. Because of their similarities, the general machine theory of doubly feed machines can be applied, however with the end effects in the linear machine taken into account.

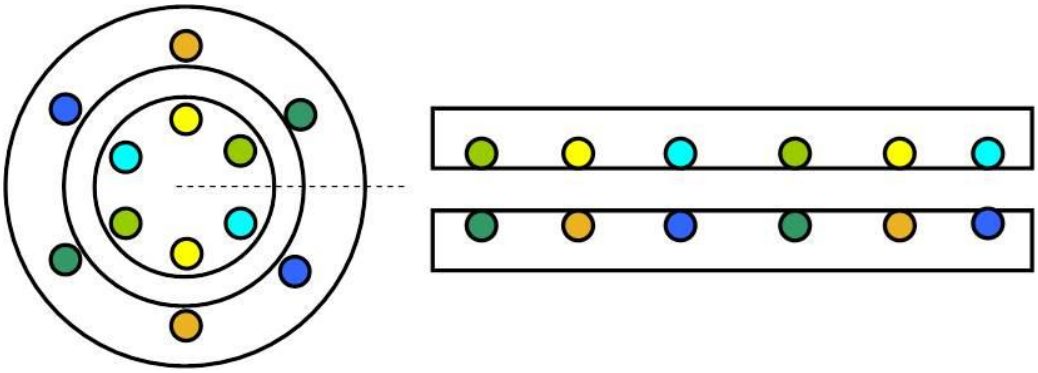

Figure 4: Regular three-phase electric motor and unfolded version (linear motor).

What this results in is a transformer with an air gap separating the two halves; a partially magnetically coupled transformer. On the receiving side, placed with the vehicle is a core containing three coils (one for each phase) with the windings in the configuration shown in Figure 5.

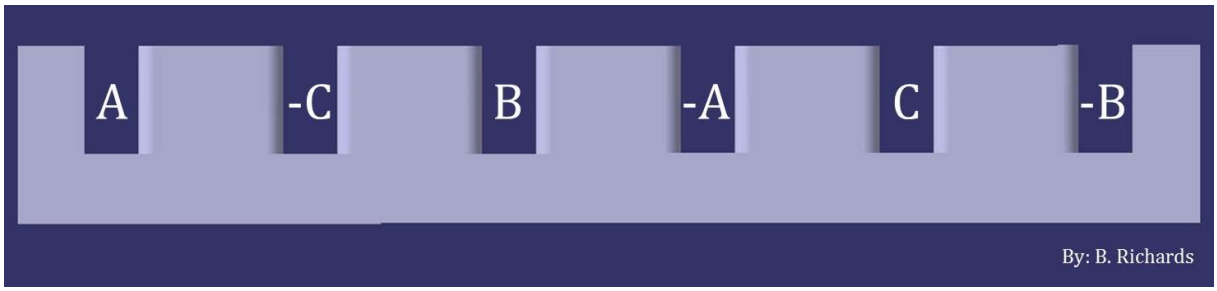

Figure 5: Side view of the receiving side core and the winding configuration.

In the road the same cores and coils are used and placed in a line in the middle of the road. A current is then driven through these coils inducing a magnetic field which passes through the coils in the receiver in the vehicle side, and induce a voltage, emf. This voltage causes a current to flow which is used to power the car's electric motor and charge the battery.

The design of the vehicle side core (or one segment of the road side core) is shown in Figure 6, and how the cores look directly above each other as when the system is transferring power is shown in Figure 7.

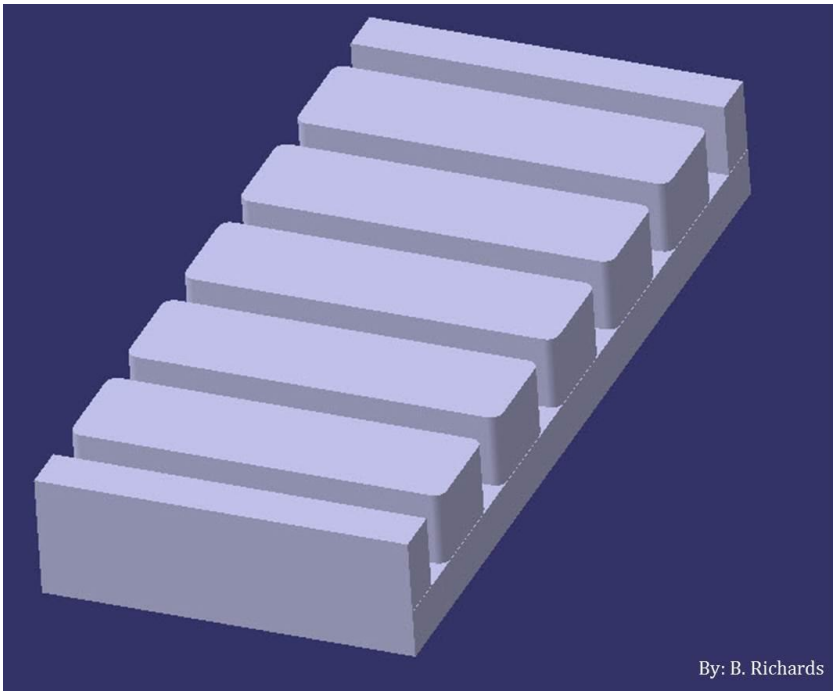

Figure 6: 3D illustration of the vehicle side core

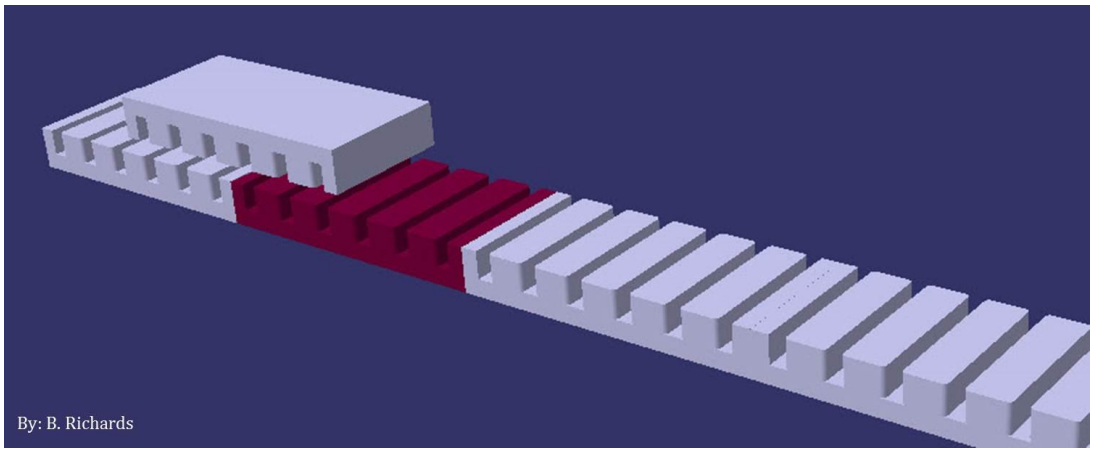

Figure 7: 3D illustration of how it looks with the vehicle side core over the road side core.

In Figure 8, the two transformer halves with windings are shown, but with only one core segment on the road side.

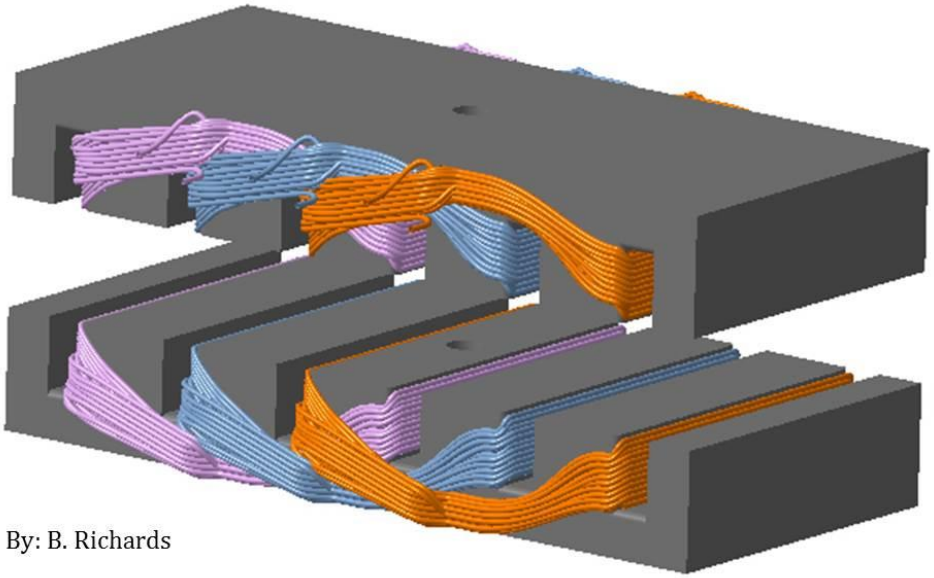

Figure 8: 3D view of the two transformer halves with windings. In the road side only one segment is shown, but in reality continues on both sides.

The physics behind inductive power transfer all come down to the relationship between current and magnetic field, which is explained by Maxwell's equations. To get a closer look at these equations and more regarding classic electrodynamics, chapter 10.1 in the appendix can be read.

2.1 Partially coupled transformer model

As the emf is a time-depending voltage in a secondary coil, Faraday's law can be rewritten to the following:

$$u_2(t) = \frac{d\psi_{12}(t)}{dt} \quad (1)$$

Here the negative sign normally accompanying the equation has been compensating for by changing the direction of the windings in the coil, see Figure 9.

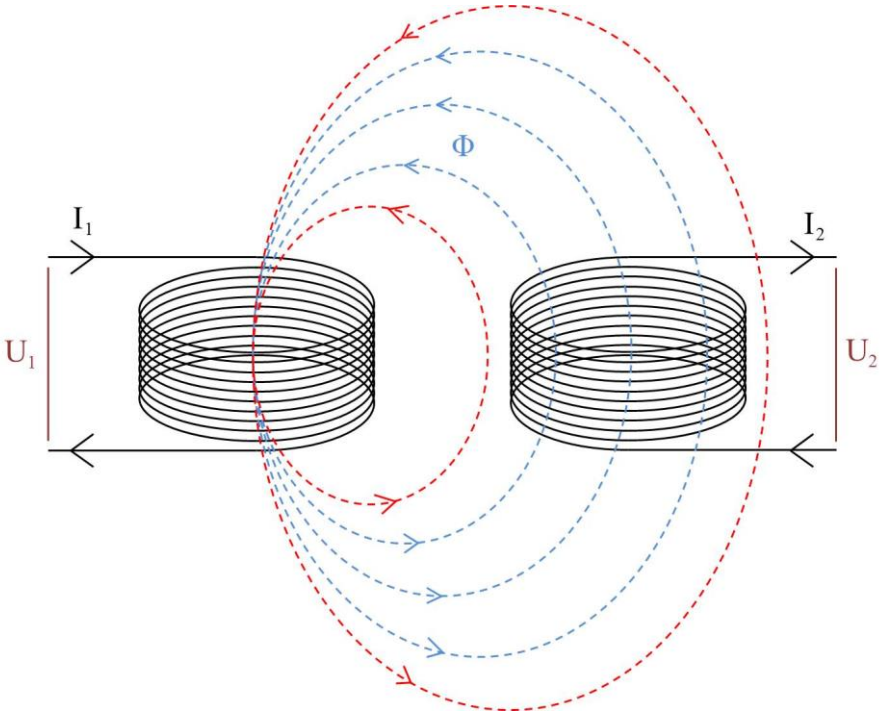

Figure 9: Visualisation of how running a current (I_1) in a coil induces a current (I_2) in a second coil if they are close enough to one another. Only part of the magnetic flux passes through the second coil and with increasing distance, this part becomes smaller.

The current in the second coil induces a magnetic field which opposes the change in mutual flux from the primary coil. This means that the total flux linkage for the second coil is defined as a combination of the mutual flux linkage (Ψ_{12}) and the self-flux linkage (Ψ_{22}).

$$\psi_2(t) = \psi_{12}(t) - \psi_{22}(t) \quad (2)$$

However just like the current in the primary coil induces a magnetic flux which partially passes through the second, the induced current induces a magnetic flux which partially passes the primary coil. This means that the total flux linkage for the primary coil is also a combination of the mutual and self-flux linkage.

$$\psi_1(t) = \psi_{11}(t) - \psi_{21}(t) \quad (3)$$

Combining these equations with equations (68) and (70), they can be rewritten in terms of inductances.

$$\psi_1(t) = L_1 i_1(t) - M i_2(t) \quad (4)$$

$$\psi_2(t) = \mathrm{M} i_1(t) - L_2 i_2(t) \quad (5)$$

By differentiating (assuming the inductances are time invariant) both sides and then using Faraday's law on the left side, these equations can be rewritten to show the relationship between the input voltage and current, and the output voltage (from the coil) and current[1].

$$u_1(t) = L_1 \frac{di_1(t)}{dt} - M \frac{di_2(t)}{dt} \quad (6)$$

[1] I.D. Mayergoyz, W. Lawson. *Basic Electric Circuit Theory*.

$$u_2(t) = M\frac{di_1(t)}{dt} - L_2\frac{di_2(t)}{dt} \quad (7)$$

If the currents are sinusoidal and steady-state, these equations can be rewritten on phasor form.

$$U_1 = j\omega L_1 I_1 - j\omega M I_2 \quad (8)$$

$$U_2 = j\omega M I_1 - j\omega L_2 I_2 \quad (9)$$

However all real inductors consist of a resistance in series with an inductance, hence the equations must be altered to incorporate these coil resistances.

$$U_1 = R_1 I_1 + j\omega L_1 I_1 - j\omega M I_2 \quad (10)$$

$$U_2 = j\omega M I_1 - R_2 I_2 - j\omega L_2 I_2 \quad (11)$$

In equation (11) the $j\omega MI_1$ part is the induced voltage in the second coil from the mutual flux linkage. The rest of the right side in the equation is voltage drops due to the impedance in the coil with no load connected (open circuit). This can also be written on matrix form.

$$\begin{pmatrix} U_1 \\ U_2 \end{pmatrix} = \begin{pmatrix} R_1 + j\omega L_1 & -j\omega M \\ j\omega M & -R_2 - j\omega L_2 \end{pmatrix} \begin{pmatrix} I_1 \\ I_2 \end{pmatrix} \quad (12)$$

The negative signs can be moved to the current in the secondary side, I_2, so that the matrix can be written as:

$$\begin{pmatrix} U_1 \\ U_2 \end{pmatrix} = \begin{pmatrix} R_1 + j\omega L_1 & j\omega M \\ j\omega M & R_2 + j\omega L_2 \end{pmatrix} \begin{pmatrix} I_1 \\ -I_2 \end{pmatrix} \quad (13)$$

Or more compact

$$\mathbf{U} = \mathbf{Z_t} \cdot \mathbf{I} \quad (14)$$

where U is the voltage vector, $\boldsymbol{Z_t}$ is the transformer impedance matrix and I is the current vector. Figure 10 illustrates equations (10) and (11).

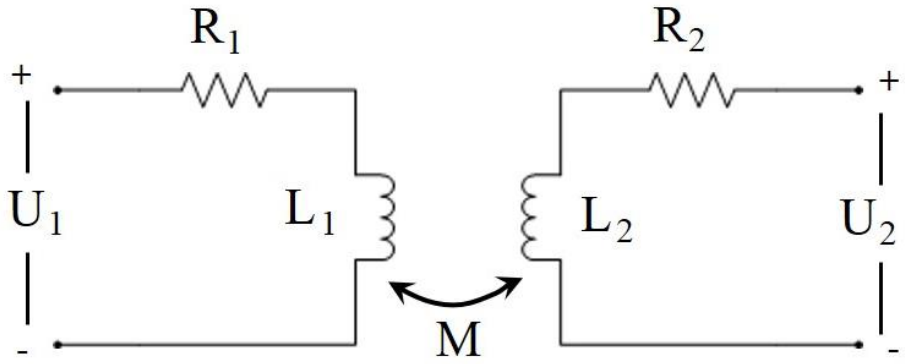

Figure 10: Circuit diagram of the mutual inductance model for a one phase system.

If a load is connected to the second coil so that the circuit becomes closed, equations (11), (12) and (14) becomes:

$$0 = j\omega M I_1 - R_2 I_2 - j\omega L_2 I_2 - R_{load} I_2 \quad (15)$$

$$\begin{pmatrix} U_1 \\ 0 \end{pmatrix} = \left(\begin{pmatrix} R_1 + j\omega L_1 & -j\omega M \\ j\omega M & -R_2 - j\omega L_2 \end{pmatrix} - \begin{pmatrix} 0 & 0 \\ 0 & R_{load} \end{pmatrix} \right) \begin{pmatrix} I_1 \\ I_2 \end{pmatrix} \quad (16)$$

$$\mathbf{U} = (\mathbf{Z_t} - \mathbf{Z_l}) \cdot \mathbf{I} \quad (17)$$

where $\boldsymbol{Z_l}$ is the load impedance matrix. Again the negative sign can be moved to I_2.

$$\begin{pmatrix} U_1 \\ 0 \end{pmatrix} = \left(\begin{pmatrix} R_1 + j\omega L_1 & j\omega M \\ j\omega M & R_2 j\omega L_2 \end{pmatrix} + \begin{pmatrix} 0 & 0 \\ 0 & R_{load} \end{pmatrix} \right) \begin{pmatrix} I_1 \\ -I_2 \end{pmatrix} \quad (18)$$

$$\mathbf{U} = (\mathbf{Z_t} + \mathbf{Z_l}) \cdot \mathbf{I} \quad (19)$$

The induced current in the secondary side can now be calculated as the induced voltage divided by the total impedance in the circuit.

$$I_2 = \frac{j\omega M}{R_2 + j\omega L_2 + R_{load}} I_1 \quad (20)$$

The expression for I_2 can then be inserted into equation (10) to give an equation for the primary side without I_2.

$$U_1 = R_1 I_1 + j\omega L_1 I_1 + \frac{\omega^2 M^2}{R_2 + j\omega L_2 + R_{load}} I_1 \quad (21)$$

This equation now shows that from the perspective of the primary side (coil), the second side circuit is seen as a frequency and geometry dependant transformed impedance.

Although the matrix in equation (16) only applies with single-phase transformers, the different relationships between the two coils is valid for all pairs in a multi-phase transformer since they all affect one another. This means that the matrix can be expanded to work on for example a three-phase transformer (both on the primary and secondary side), which is the most effective way to transfer energy. For the three-phase equations, see chapter 10.3 in the appendix.

In the $\boldsymbol{Z_t}$ matrix, each element contains a corresponding value from an inductance matrix, denoted $\boldsymbol{M}$ in the matrix. Here $\boldsymbol{M_{ii}}$ is self-inductance and $\boldsymbol{M_{ij}}$ equals $\boldsymbol{M_{ji}}$. Just like with the 2x2-matrix, since loads are connected to the secondary side the total voltage in these circuits sums up to zero. Although all mutual inductances are positive, calculating it through simulations using equation (70) in the appendix, the phase shift between the current in one phase and the magnetic flux in the same or another adds a sign to the mutual inductance (positive or negative). This indicates if a current in- or decreases the induced voltage in one of the phases.

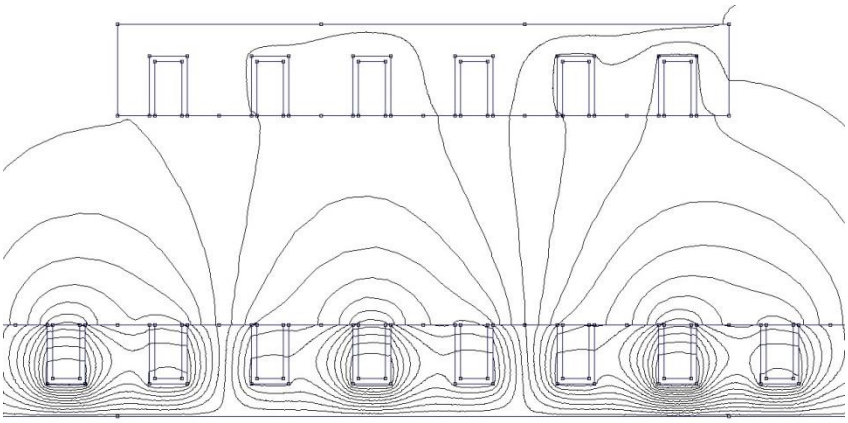

Figure 11: Magnetic field lines in the primary and secondary core due to current in the primary side coils.

2.2 Design parameters

As seen there are several design parameters which determine how much energy can be transferred from the road to the vehicle, and all these need to be considered while designing the system. As previously seen in equation (1), the induced voltage in the receiver (in the case of one coil per side) equals $j\omega MI_1$ (see Figure 12) and if the distance between the coils is increased, the mutual inductance decreases which mean less voltage induced and power transferred. To counteract this, the frequency can be increased to maintain the desired voltage level. However when the frequency is increased the losses are also increased so even though a high frequency is both desired and necessary, the losses must be taken into consideration so that the efficiency does not suffer and becomes too low because a too high frequency was used.

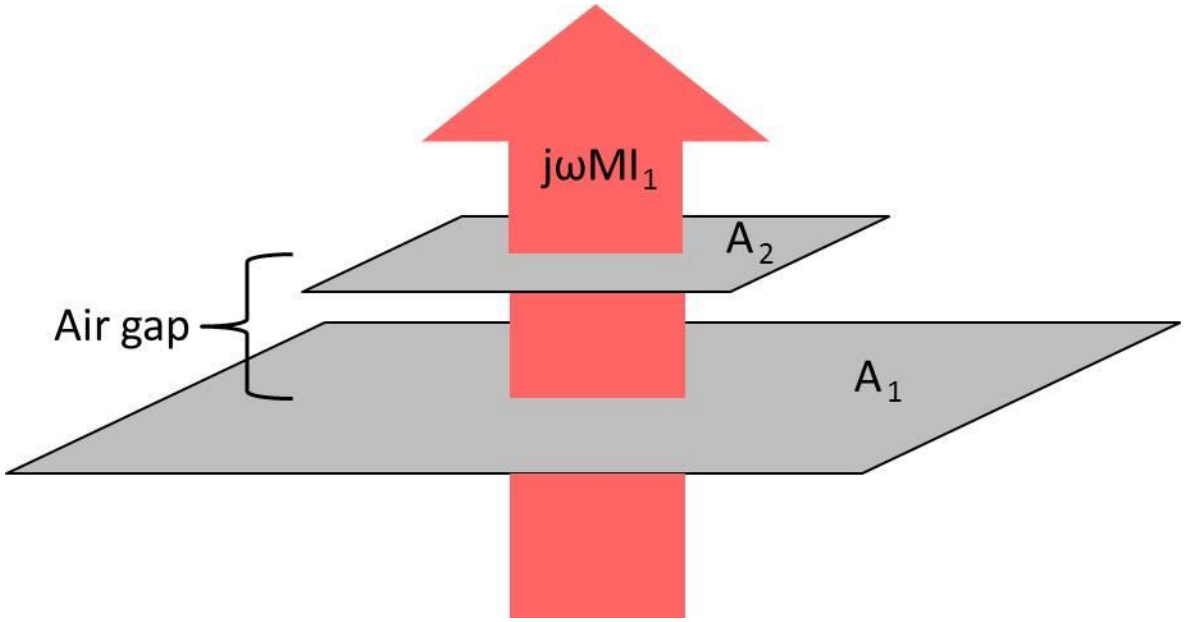

Figure 12: Some of the design parameters illustrated.

Another parameter which is also a question of balance is the size of the coils used. When the cross sectional area is increased in the primary side the magnetic flux increases and when the same is done in the secondary, the amount of flux going through it increases. However the bigger the coils are made, the more they cost and beyond the technical aspect, the economical is a determining factor.

Together with the size of the coils come the core material and the number of turns in each coil. The core should have a high relative permeability, which increases the ability to support the formation of a magnetic field within itself. However different materials can handle a different amount of magnetic field and frequency and are differently vulnerable for losses resulting from high frequencies.

The magnetic flux generated by the primary side and the flux linkage experienced by the secondary side both increase with the number of turns in the coils. However the size of the coils and the conductors limits how many turns each coil can have. In addition, the material of the conductors determines the losses, but the material with the better conductivity may be more expensive so this creates another question of balance.

2.3 Complex power compensation

A high self-inductance and low coupling inductance result in more voltage across the reactance and less over the coupling inductance, see equation (21). The reactive voltage drop causes a delay between the voltage and the current which introduces reactive power. This power does no work and only leads to a lower power factor.

To keep the power factor as high as possible in a system with inductances it is necessary to work with resonance. An inductance cause the current to lag 90° compared to the voltage whereas a capacitor leads the current 90°, expressed by the equations for their impedances.

$$Z_L = j\omega L \quad (22)$$

$$Z_C = \frac{1}{j\omega C} \quad (23)$$

If these impedances can be matched the phase shifts cancel each other out. To determine the value of the compensation component (in this case a capacitance) the inductance together with the frequency at which the system works must be known and is done as shown below:

$$\omega L = \frac{1}{\omega C} \quad (24)$$

This gives the value of the capacitance:

$$C = \frac{1}{\omega^2 L} \quad (25)$$

This method of compensating the phase shift should be used on both the primary and the secondary side to make sure that the whole system is in resonance. Using this method on the primary side furthermore decreases the current absorbed by the converter, which leads to reduced switching losses.

The resonance angular frequency is defined as:

$$\omega = \frac{1}{\sqrt{L \cdot C}} \quad (26)$$

The compensation capacitances can be connected in four different basic topologies, shown in Figure 13, Figure 14, Figure 15 and Figure 16 respectively, and are the following:

- Series in primary – series in secondary.
- Series in primary – parallel in secondary.
- Parallel in primary – series in secondary.
- Parallel in primary – parallel in secondary.

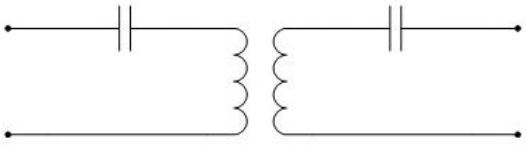

Figure 13: Series-series compensation.

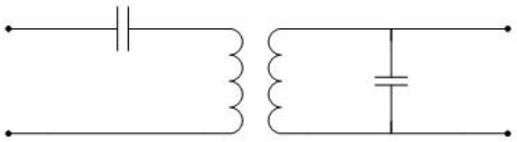

Figure 14: Series-parallel compensation.

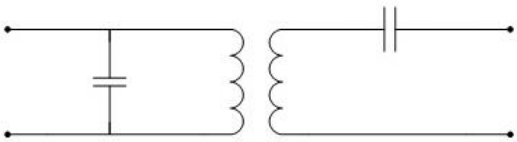

Figure 15: Parallel-series compensation.

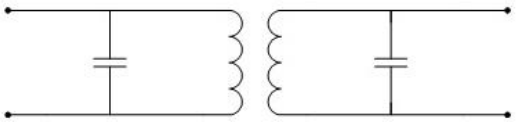

Figure 16: Parallel-parallel compensation.

Connecting a capacitor in series makes it work as a controllable voltage source, which is especially useful in AC transmission lines. All transmission lines contain series inductances and on long lines with large currents these cause voltage drops. The series capacitor decreases the effect of the inductances leading to lower losses and better power transfer.

For the series option the total impedance (excluding the resistances) is the sum of the individual impedances.

$$Z_s = Z_L + Z_C \quad (27)$$

or

$$Z_s = \frac{j(\omega^2 LC - 1)}{\omega C} \quad (28)$$

At resonance frequency the series impedance goes to zero.

$$\lim_{\omega \to \frac{1}{\sqrt{L \cdot C}}} Z_s = 0 \quad (29)$$

If the capacitor is instead connected parallel to the inductance, it works as a controllable current source. As previously stated the inductance lags the current, whereas the capacitance leads it, so when a capacitance is connected in parallel it draws current leading the voltage. This means that the net result is that the circuit only draws active power from the source leading to an improved power factor[2].

Using the parallel compensation alternative, the total impedance (excluding the resistances) is calculated as the product divided by the sum of the two individual impedances.

$$Z_P = \frac{Z_L Z_C}{Z_L + Z_C} \quad (30)$$

or

$$Z_P = \frac{\omega L}{j(\omega^2 LC - 1)} \quad (31)$$

At resonance frequency the parallel impedance goes to infinity.

$$\lim_{\omega \to \frac{1}{\sqrt{L \cdot C}}} Z_P = \infty \quad (32)$$

From a physical point of view all four combination of resonance compensations are viable options, so there is no real need to choose one of the configurations as a standard.

2.4 Hover techniques

Air bearing is a technique which uses air to lift an object. There are three different types of air bearing for different applications, air cushioning, rigid air bearing and complaint air bearing.

2.4.1 Air bearing

2.4.1.1 Air cushioning[3]

Air cushioning is the method hover crafts uses. A hover craft is a vehicle able to drive over most surfaces, and it utilises air as both propulsion and lifting. Under the hull is a skirt which acts as a constraint for the air pumped under it, leading to an increased air pressure inside it big enough to lift the craft. To facilitate the movement across the surface it is traveling over and decrease wear and tear through friction, the skirt has holes in the underside which let some of the air out (see Figure 17). This means that air has to be constantly pumped into the skirt to maintain the required pressure to achieve lift. To calculate the required air flow and the size of the holes for a hovercraft, the following method can be used.

[2] Wikipedia (2013) Flexible AC transmission system.
[3] CUA (2008)

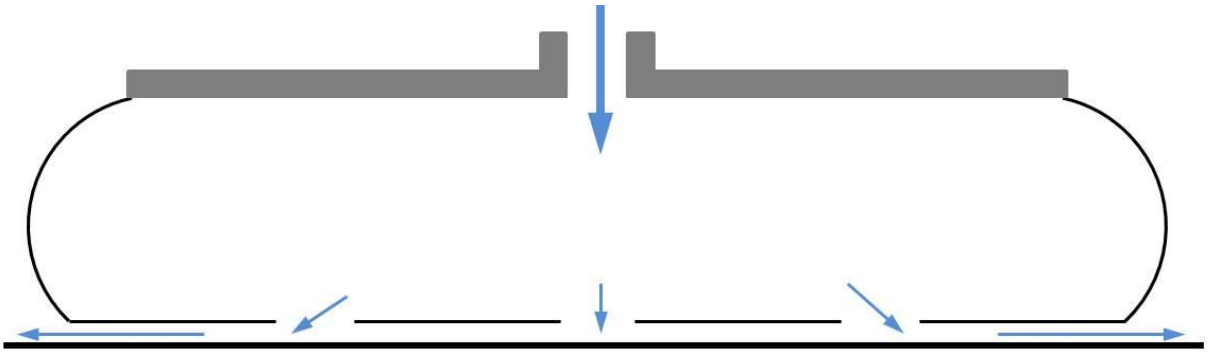

Figure 17: Cross sectional image of air cushioning, with the air flow marked.

The air cushion pressure (P_{cus}) needed under the hull equals the gravitational force exerted on the vehicle by the Earth divided by the hovercraft footprint (the area of the underside of the hull).

$$P_{cus} = \frac{m \cdot g}{A} \quad (33)$$

Bernoulli's equation can then be used to calculate the escape velocity of the air from under the skirt through the gap made from the hovering.

$$V_{esc} = D_c \sqrt{\frac{2P_{cus}}{\rho_{air}}} \quad (34)$$

ρ_{air} is the density of the air, and *Dc* is the discharge coefficient and is usually approximated to a value of 0.53. This air escapes through the area created by the circumference of the hovercraft footprint and the chosen hover gap height.

$$A_{gap} = L \cdot h \quad (35)$$

where *L* is the circumference and *h* is the hover gap height (the distance between the surface and the skirt, not the hull).

The flow rate (*Q*) of the air escaping through the hover gap is calculated using the general formula of flow rate.

$$Q = A_{gap} \cdot V_{esc} \quad (36)$$

"The proper design pressures for a skirt require at least 20 % more pressure inside the skirt than the pressure directly lifting the craft over the area of the underside[4]." This is important since if the air pressures were equal, the craft would most likely not hover since the escaping air would not result in any lift. So the pressure inside the skirt (P_{bag}) should, with some margin, be 30 % higher than the air cushion pressure.

$$P_{bag} = 1.3 \cdot P_{cus} \quad (37)$$

From here the total size of the holes (A_{net}) in the underside of the skirt can be determined; regardless of how many are chosen.

[4] J. Perozzo. *Hovercrafting as a Hobby*, p. 27.

$$A_{net} = \frac{Q}{C \cdot \sqrt{\frac{2}{\rho_{air}}\left(P_{bag} - P_{cus}\right)}} \quad (38)$$

where *C* is a typical flow loss value of 0.86. The last part is to obtain the size of each individual hole, which is calculated as the total area needed, divided by the number of holes (*N*), which can be chosen freely.

$$A_{hole} = \frac{A_{net}}{N} \quad (39)$$

An advantage with this solution is that it can handle big variations because of the high ground clearance. However they require a high air flow which means high power consumption. The load carrying is limited by the relatively low air pressure the skirt can handle[3].

2.4.1.2 Rigid air bearing[5]

The second method is the rigid air bearing and this option can support very heavy loads, over 19 tonnes per m^2. These do not have any form of material maintaining a certain air pressure, but instead an extremely thin air film is forced between the support surface and the ground, see Figure 18. The air film is usually only a few tens of µm thick which demands a very flat surface and only the smallest of variations can be handled. However the advantages are, in addition to the ability to support heavy loads, that they require little power and produce low noise.

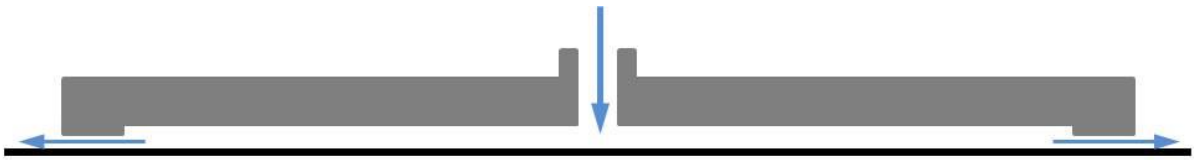

Figure 18: Cross sectional image of rigid air bearing, with the air flow marked.

2.4.1.3 Complaint air bearing[5]

The last method is the complaint air bearing which combines the two previous methods. When air is pumped into its flexible diaphragm it unfolds into a cone, seen in Figure 19. The air inside the diaphragm then escapes through holes into the formed cone in a way so that the air pressure is the almost equal both in- and outside the diaphragm. The air inside the cone then escapes outward, under the footprint area where the air gap height is very small.

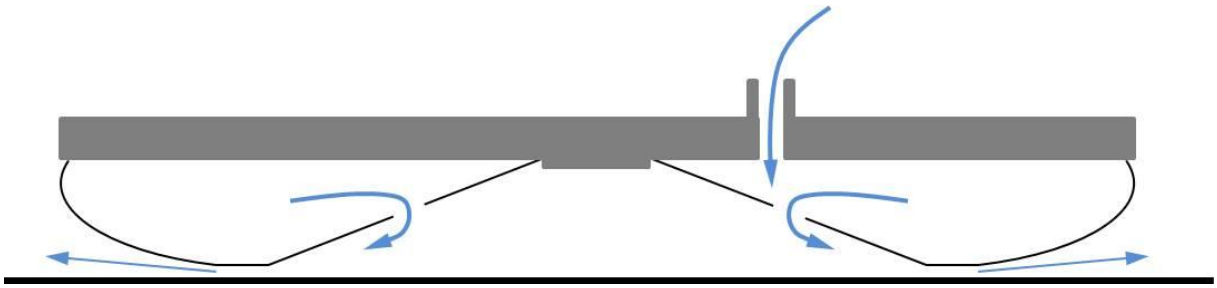

Figure 19: Cross sectional image of complaint air bearing, with the air flow marked.

When the air escapes through this narrow gap its speed increases, causing the pressure to drop slightly in accordance with the Bernoulli effect. This causes the diaphragm and the whole

[5] Airfloat (2012 May) *How Air Bearing Works*

construction to lower, creating a self-regulating clearance gap. This makes it possible to handle smaller variations in the ground, giving it more possibilities than the rigid option.

Complaint air bearing devices can handle loads up to almost 10 tonnes per m^2 and has a low power requirement and makes little noise.

The material used for the diaphragm is made durable and because air bearing is nearly frictionless, the wear and tear under normal conditions is minimal.

Estimating the required air flow is difficult and every application has its own solution. However for a system 254 mm (10 inches) across on poor floor conditions require a flow of less than 6 l/s[6].

2.4.2 Magnetic levitation

When two magnets are brought together they either attract or repel. Depending on if the poles facing each other are the same or the opposite. This force approximately decreases with the inverse of the squared distance between them, meaning the force quickly loses its impact when the distance is increased[7].

The same is true for electromagnets[8], and since the induced current in the receiving side of the transformer produces a magnetic field which opposes the field from the primary side, the result is repulsion. However in the case of a multi-phase system, the induced current depends on the magnetic flux from all other coils, meaning the produced field does not strictly repulse the primary side. Instead it attracts some of the coils and repels others, and the total force becomes weaker, regardless of if the force causes attraction or repulsion.

2.5 Shielding

The magnetic field from a current loop decreases roughly with the inverse of the cube of the distance on the axis to the normal of the loop. However with a strong magnetic source the field strength cannot be ignored since there are limits for how much magnetic field a person may be exposed to.

The limits are set to only protect against the effects which are scientifically proven, and because the proofs are mostly considered inadequate, the limits are set so they only offer a minimal protection.

In Sweden the recommendations from EU and WHO are used and these states that in the frequency range of 2 to 400 kHz, the limits are between 6.25 and 2.3 μT. The higher the frequency, the lower the limit is set due to the fact that faster variations of the field affect humans more[9]. As a comparison the Earth's magnetic field at ground level ranges from 25 to 68 μT[10]. In Figure 20, the magnetic field density from the road side transformer half is shown when the primary coils consists of 20 turns and are excited with a 100 A peal current.

[6] Airfloat (2013 January) *Minimum Estimated Air Consumption for Air Bearings*
[7] F.P. Gram (2003, January 23) *Magnetic Field and Forces*.
[8] Wikipedia (2013) Electromagnet.
[9] Vågbrytaren Stockholm (2012, February 9) *Gränsvärden för elektriska och magnetiska fält samt elektromagnetiska vågor – strålning*
[10] Wikipedia (2013) Earth's magnetic field.

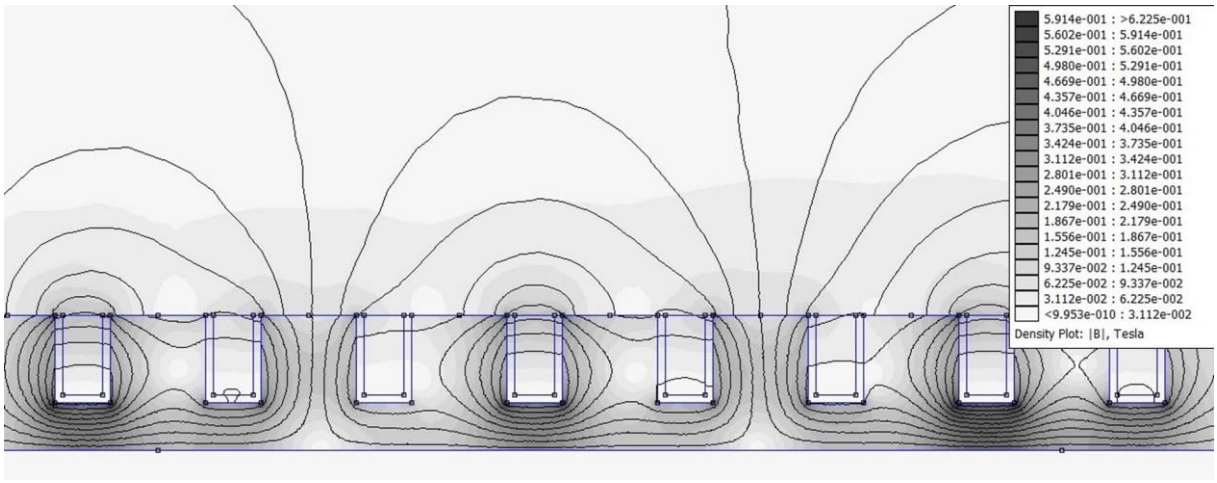

Figure 20: Magnetic field density from the road side transformer half.

In contrast to electric fields which can be blocked, magnetic fields cannot and instead materials which attract the magnetic field are used as shields. These materials need to have a high magnetic permeability so that they can draw the field lines in and provide them with a path around the shielded volume.

This solution is called passive shielding, but there is an alternative which uses active shielding technique. This method is based on the use of electromagnets which produces an opposite magnetic field that cancels out the field outside the desired volume[11].

2.6 Losses

Losses are an unavoidable part of any physical event where energy conversion takes place and in the case of transformers these losses can be categorised into two main groups, losses due to conductor resistance and losses happening in the transformer core. In addition, the transistors used for the dc-ac conversion have switching losses occurring when a transistor switches from conducting to being closed.

2.6.1 Conductive losses

The most important aspect of how well a material can conduct a current is its electrical resistivity, denoted ρ. Also known simply resistivity, this parameter tells how strongly a material opposes an electric current. All materials can be divided into three categories, conductors, semiconductors and insulators. Metals are examples of good conductors and usually have a resistivity in the order of 10^{-8} to 10^{-7} Ω·m, and the lower this value is, the better the material is at conducting the electrons' movement. The most commonly used conductor is copper which has a resistivity of $1.68 \cdot 10^{-8}$ Ω·m at normal room temperature[12]. In larger applications using copper is too cost inefficient and instead aluminium can be used, which has a resistivity of $2.82 \cdot 10^{-8}$ Ω·m at room temperature[13].

The actual DC-resistance of a material depends on, except the already mentioned resistivity, the length of the conductor and the cross sectional area.

[11] Wikipedia (2013) Electromagnetic shielding.
[12] Wikipedia (2013) Copper.
[13] Wikipedia (2013) Aluminum.

$$R = \rho \cdot \frac{l}{A} \quad (40)$$

where *l* is the length of the conductor and *A* is the cross sectional area. If the conductor is wound into an N-turn coil the resistance increases with the number of turns squared, when considering the average length of the coil and the total conductor area A_c[14].

$$R = N^2 \cdot \rho \cdot \frac{l}{A_c} \quad (41)$$

Switching from a low to a high frequency changes the resistance so that it increases because of skin effect and proximity effect.

Skin effect is a tendency which alternating currents have due to self-inductance, to redistribute its current density so that it is largest near the surface of the conductor, instead of being homogenously distributed across the conductor cross sectional area[15]. This leads to more current flowing through a smaller area which increases the resistance, in accordance to equation (40). As previously discussed, an alternating current generates a changing magnetic field which in turn induces eddy currents. These currents oppose the main current, causing it to amass near the surface, or skin, of the conductor since they are strongest in the middle of the conductor.

The parameter used for describing this effect is called skin depth, denoted δ, and gives the depth from the surface at which the current density has decreased to *1/e* (about 0.368) of the surface value. The skin depth is calculated as the following equation shows:

$$\delta = \sqrt{\frac{2\rho}{\omega\mu}} \cdot \sqrt{\sqrt{1 + (\rho\omega\epsilon)^2} + \rho\omega\epsilon} \quad (42)$$

where ω is the angular frequency, μ is the absolute magnetic permeability of the conductor and ϵ is the electric permittivity. However for frequencies much smaller than $1/\rho\epsilon$ the equation can be approximated with

$$\delta = \sqrt{\frac{2\rho}{\omega\mu}} \quad (43)$$

For copper this limit frequency is in the order of 10^{18} Hz, so the approximation works well in this case. The AC-resistance caused by the skin effect can then be approximated with

$$R \approx \frac{L\rho}{\pi(D - \delta)\delta} \quad (44)$$

where *D* is the diameter of the conductor[16].

To reduce this effect, a special wire called Litz wire can be used, which consist of several individually insulated strands, usually twisted or woven. Because each strand only carries part of the total current and is thinner than the skin depth, it does not suffer from the skin effect as much as a regular wire. In

[14] Wikipedia (2013) Electrical resistivity and conductivity.
[15] N. Mohan, T. Undeland, W. Robbins. *Power Electronics, 3rd rev edition*.
[16] Wikipedia (2013) Skin effect

addition, the weight is reduced and the lowered AC-resistance leads to less loss, which means decreased operating temperature and a higher efficiency[17].

Proximity effect is the other consequence of alternating current, which is especially prominent when several conductors lie close to one another, such as in a coil. Just as with the skin effect it is the induced magnetic field creating the problem. The field from each wire affects the wires around it and changes the current density distribution because of induced eddy currents. The result of this is that the current density in a conductor is at its highest in the areas furthest from the other conductors around it. Just like with the skin effect, the AC-resistance due to the proximity effect increases with higher frequencies.

$$R_{AC} = R_{DC}\left(Re(M) + \frac{(m^2-1)Re(D)}{3}\right) \quad (45)$$

where *M* and *D* are factors depending on the geometrical properties of the conductors, the frequency and the resistivity[16] (full explanation in chapter 10.4 in the appendix).

Using Litz wire helps minimising this increase in resistance as well. Since Litz wires are twisted so that each strand's location is changed from centre to edge throughout the length of the wire, the proximity effect affects each strand the same, meaning each strand carries the same current.

The actual power loss caused by the conductor's resistance is then calculated by multiplying it with the square of the current through it, or dividing the square of the voltage with it.

$$P = R \cdot I^2 = \frac{U^2}{R} \quad (46)$$

2.6.2 Core losses

It is not only the conductors which get affected by the magnetic field, but also the core of the transformer. The losses associated with the core can be categorised into hysteresis and Eddy current losses. These losses depend on the physical properties of the core material, its design and the frequency of the current and therefore the magnetic field density through the material.

The core of a transformer consists of a ferromagnetic material, which is a material that has magnetic dipoles (can be compared to small permanent magnets) randomly arranged inside it. The net resultant magnetic field for these materials is zero; however when an external magnetic field influences the material, the dipoles rearrange to follow this field. When the external magnetic field no longer affects the material most dipoles yet again get positioned randomly, but some remain in the new position leaving the material slightly permanently magnetised. To counteract this, an opposing magnetic field needs to be applied, meaning more work is required to change the net resultant magnetic field to the other direction. This is what happens when running an alternating current through a transformer, and for every cycle some energy is consumed by this process and is known as hysteresis losses.

$$W_h = K_h f B_m^{1.6} \quad (47)$$

[17] F.E. Terman. *Radio Engineers' Handbook*.

where W_h is the hysteresis loss, K_h is a hysteresis constant, f is the frequency of the current and B_m is the maximum magnetic flux density.

The magnetic field (see Figure 21) does not only change the directions of the dipoles in the core material, but also induces Eddy currents. These currents cause resistive losses in the core which translates to heat.

$$W_e = K_e f^2 K_f^2 B_m^2 \quad (48)$$

where W_e is the Eddy current loss, K_e is a Eddy current constant and K_f is a form constant which can basically account the geometric thickness of the core laminates or powder particle.

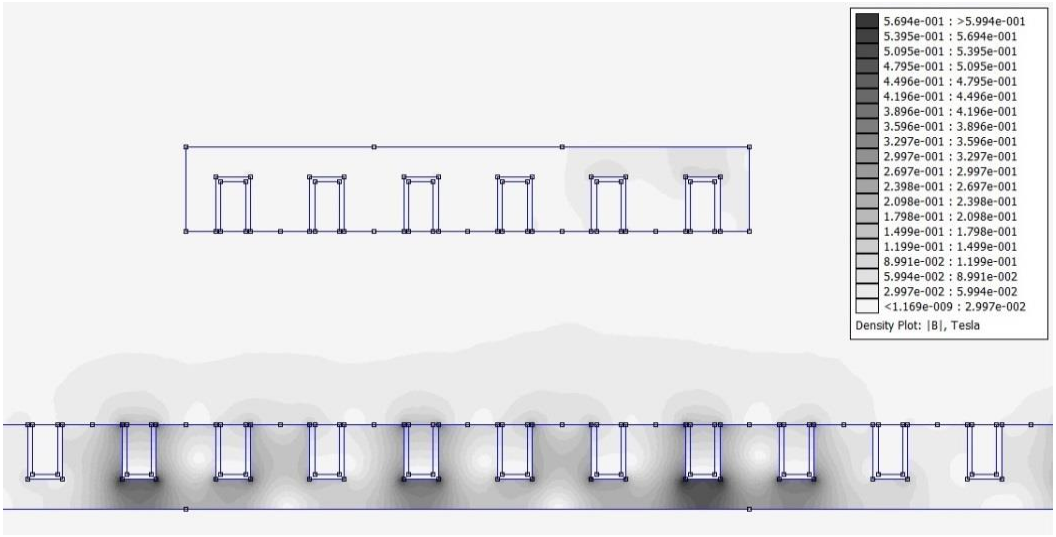

Figure 21: Magnetic field density in the primary and secondary core due to 100 A current in the primary side coils.

The effect of Eddy currents can be reduced by using materials with low electrical conductivity or by reduced conducting area. High frequency cores are therefore usually made of powder or stacks of sheets of the core material, known as laminations. Each sheet is separated by insulation and since the electrons cannot cross the insulation which prevents the current from taking wider paths around the core, see Figure 22. The more lamination sheets per area, the more effectively the Eddy currents are suppressed.

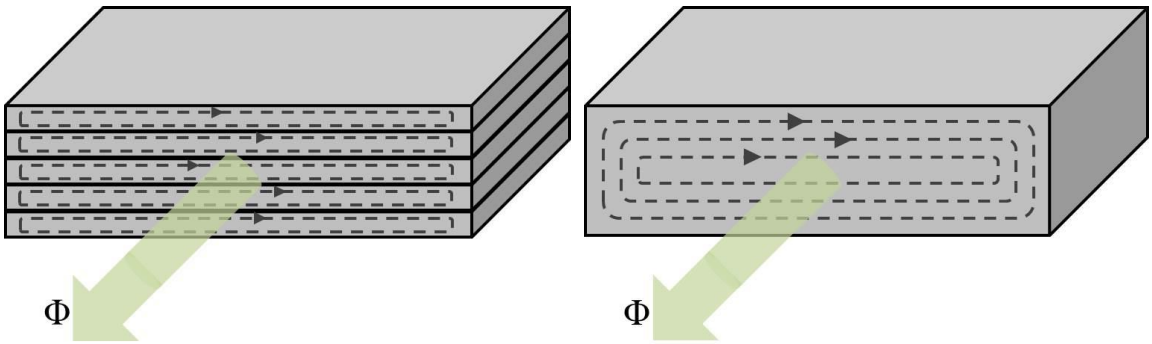

Figure 22: The effect for Eddy currents when using laminates versus solid block.

From equation (47) and (48) it becomes clear that the Eddy current losses are the greatest problem with high frequencies because it increases with the frequency squared compared to the hysteresis losses which increases linearly with the frequency.

These equations are often difficult to use because of the problems with obtaining the correct constants, and alternative methods such as obtaining a material's loss per mass at the specific frequency[18].

2.6.3 Switching losses

When transistors and diodes go from blocked to conductive state, and vice versa, there are always losses. There are also some conduction losses, but these are negligible most of the time since the components' inner resistances are very small.

When a transistor is turned on, the drain current starts to increase to its maximum value while the drain-source voltage goes down. Because there is a small inner resistance when the transistor is conducting, the voltage does not go all the way down to zero, which leads to conduction losses. When the transistor closes again the opposite happen; the voltage starts to increase again while the current drops to zero (see Figure 23). The total losses for a transistor are the sum of the switching losses and conduction losses:

$$P_{sw} = \frac{V_D \cdot I_D \cdot f_s}{2} \cdot \left(t_{on} + t_{off}\right) \quad (49)$$

$$P_{on} = D \cdot I_D^2 \cdot R_{DS} \quad (50)$$

$$P_{tot} = P_{sw} + P_{on} \quad (51)$$

where f_s is the switching frequency, t_{on} is the time it takes for the transistor to switch on, t_{off} is the time to switch it off, D is the duty cycle and R_{DS} is the transistor resistance when conduction. Since this happens twice every period, the total loss increases quickly with the frequency.

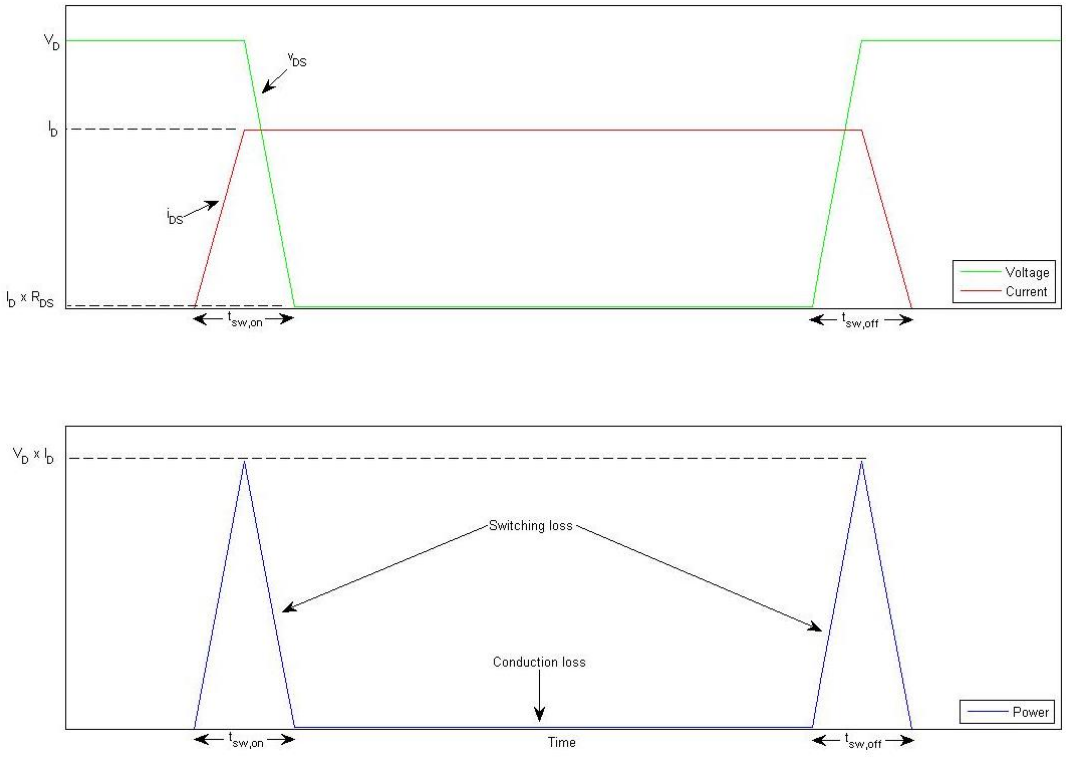

Figure 23: Losses for a MOSFET during hard switching.

[18] Electrical Engineering.

2.7 Road side

In Sweden the bigger roads' upper three layers consists of wearing course (45 mm), binder course (50 mm) and base course (80 mm) as shown in Figure 24, and it takes 6-10 years before the road needs new wearing course[19].

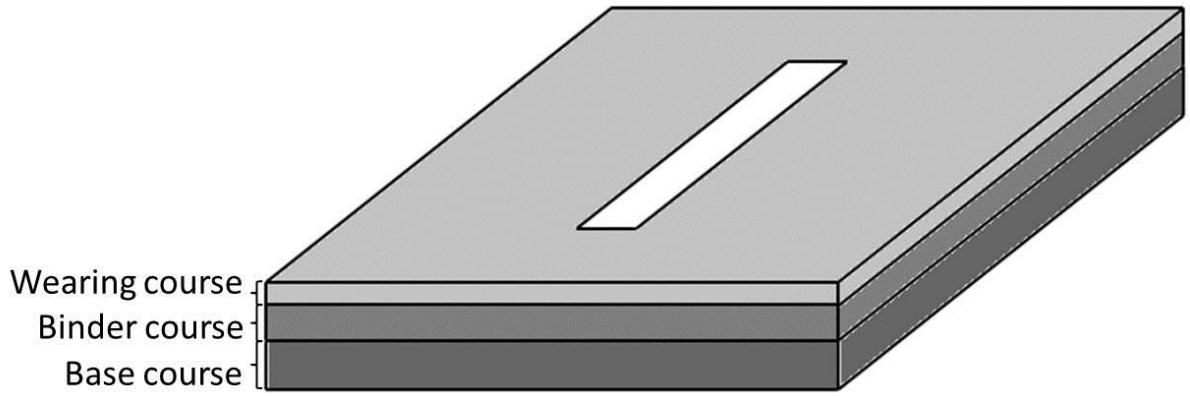

Figure 24: The three upmost layers of a Swedish highway.

As of the beginning of 2013, there is 6500 km of European highways in Sweden, and also an additional 8900 km of national highways[20].

3 Existing solutions

3.1 Stationary inductive power transfer

Transferring power wirelessly is nothing new and today there already exist many products which are being charged without being connected to the AC outlet with a cord. Examples on this are torches, electric toothbrushes, remotes, slippers with electronic warming and an application which is relatively new but is rapidly increasing in popularity, cell-phone charging.

Another field in which much research is done to explore the possibilities with wireless power transfer is the transport industry. As discussed in the introduction, the need for electric vehicles is going to increase because of diminishing oil reserves and environmental awareness, but their limitations regarding range and time needed to recharge are the biggest hindrances to an electrically driven vehicle fleet. Transferring power from the road while driving would solve both of these problems, and transferring the power wirelessly is one of the possible solutions. It would also be possible to charged parked vehicles this way.

3.2 KAIST and OLEV Technology

KAIST (formally the Korean Advanced Institute of Science and Technology) has developed a method for wirelessly transferring power to busses. Their method consists of having two parallel conductors in segments, which are turned on only when a bus is driving over them, see Figure 25. This protects from subjecting people around the power lines with magnetic field when no bus is near, and increases the efficiency. The receiver is put under the bus and is located 20 cm above the road, whereas the power lines in the road are placed 15 cm below the surface, resulting in a total distance

[19] K. Lind, Trafikverket (2013 February 20)
[20] Trafikverket (2013 February 2013) *Sveriges vägnät*

of 35 cm. Because of the distance the pickup modules need to be quite large (width of 80 cm) and several modules are needed to be able to make the transfer of 100 kW possible. The system is one phase and runs a 200 A current with the frequency 20 kHz and has an 80 % efficiency. Because of the continuous power transfer the need for batteries can de decreased to 20 % of an electric bus not capable of wireless charging. In addition, only part of the bus route needs to have these power lines and where there are none, the battery suffices. Together with OLEV Technologies, this solution is being commercialised and now exists in a few places in South Korea[21] [22] [23].

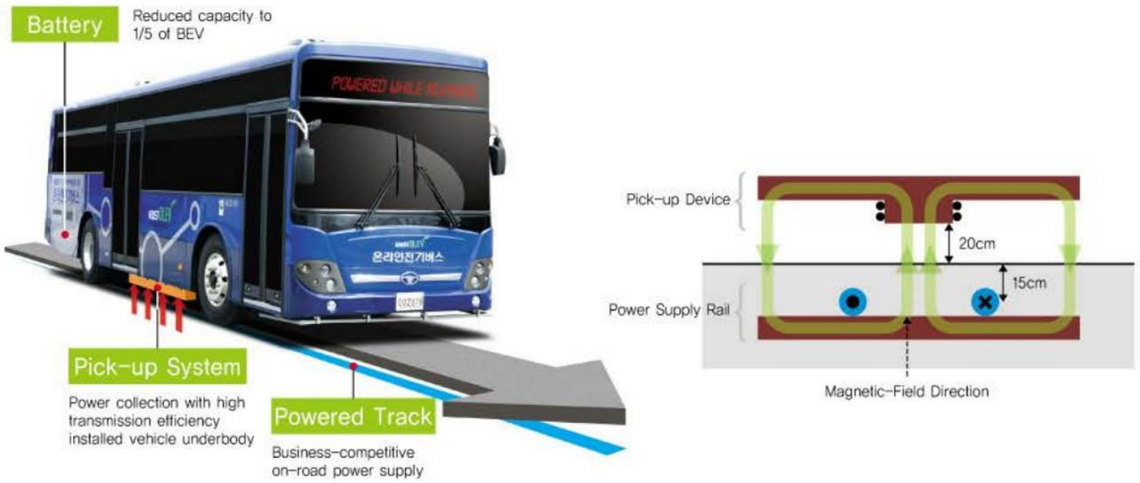

Figure 25: The KAIST/OLEV Technology solution[23].

3.3 PRIMOVE

Another company which also works to make wireless charging while driving a viable option is PRIMOVE, the e-mobility unit within Bombardier. PRIMOVE does not only work for wireless charging of busses, but for cars and trams as well. For busses the planned stops are ideal locations for charging the batteries and can be distributed among the stops to minimise the need for wayside infrastructure. If there is a steep hill along the bus route, additional dynamic charging sections can be installed to give extra energy and avoid the battery losing too much power. Using this solution for trams provides an extra bonus since no cable wires are needed and therefore do not cause any visual pollution. Just like with busses, a mix of static and dynamic charging works best, and minimises the need for batteries and wayside infrastructure. PRIMOVE's solution uses a three-phase system which is divided into segments, to avoid unnecessary magnetic field around the roads and maximise its efficiency. An antenna is used to communicate with the road so that only the segments directly under the vehicle are on. In the vehicle is a control unit which decides how to best utilise the power, for charging of the batteries, for propulsion or for both. PRIMOVE's technology is already used in Augsburg, Lommel and Braunschweig[24].

[21] OLEV Technologies (2013) *Background*.
[22] OLEV Technologies (2012 August) *Magnetic Field Design for Low EMF and High Efficiency Wireless Power Transfer System in On-Line Electric Vehicles*
[23] OLEV Technologies (2012 August)
[24] PRIMOVE (2013) *The technology behind primove*.

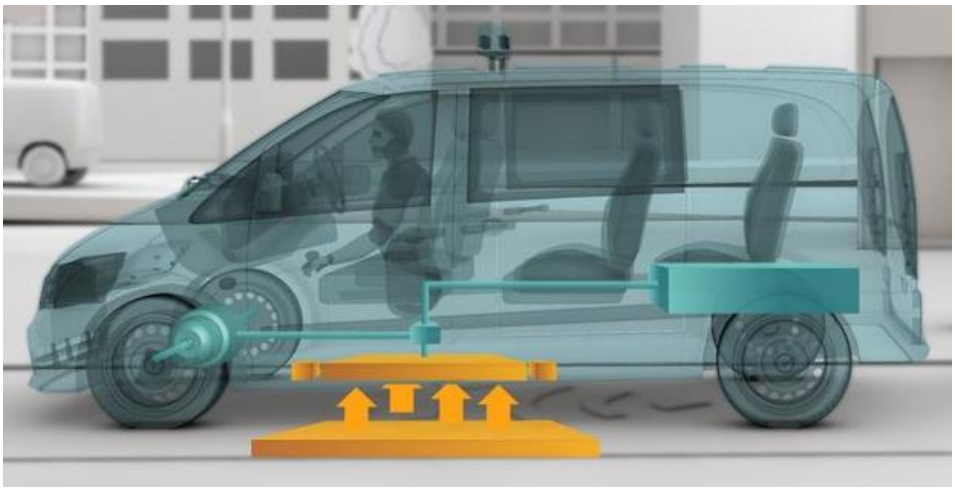

Figure 26: The PRIMOVE solution for cars[25].

4 Evaluation model

The model used in the simulations is based on a three-phase linear motor, with the receiver having one coil per phase. Different combinations of design parameters have then been tested to create a system able to transfer the power specified by the objectives.

The model was tested with two different air gaps, one for which a traditional road design was assumed and one were an unspecified and unconventional scenario was imagined.

The first takes into account that a Swedish highway has a 45 mm thick wearing course, which the core and coils is placed directly under so that they are not be damaged in any way by traffic. In addition, the air bearing system was assumed to require 30 mm which would put the vehicle side coils 75 mm above the road side coils.

For the second option the idea is to place the coils level with the wearing course and with only a very thin barrier between them and the air above to road. This barrier needs to be smooth enough so that is does enable an air bearing system which could be closer to the road, but also with enough friction for motorcyclists to cross safely. An example of how this can be done is by using titanium, which is non-ferrous and can be finely textured using laser welds during manufacturing and maintenance (as per suggestion by B. Richards). With this configuration the total air gap was assumed to be 30 mm.

4.1 Specifications

The core material was chosen to be supermalloy, which is a metal alloy composed of 79 % nickel, 16 % iron and 5 % molybdenum. Supermalloy has a very high magnetic permeability and low coercivity, giving the alloy the property of having magnetic fields flowing through it easily. It is also a soft magnetic material which means that once the magnetic field is removed, it does not stay magnetised[26]. From the composition, the alloy's density is estimated to 8.8112 g/cm^3, or 8811.2 kg/m^3.

[25] Primove (2013) *PRIMOVE automotive*
[26] Wikipedia (2013) Supermalloy

The configuration of the cores (vehicle and road side respectively) and the coils in them are listed in Table 1, Table 2 and Table 3. The wires are made of copper and are shaped as rounded squares with the side 100 mm. The fill factor determined by the model is circa 60 %.

Table 1: Core dimensions for the receiver seen from the side as in Figure 5.

Core dimensions	Width [mm]	Depth [mm]	Height [mm]
Teeth	27	100	20
End teeth	13.5	100	20
Back	222	100	13
Slot	10	100	20

Table 2: Specifications for the vehicle side coils and core in the basic solutions used during the simulations.

Vehicle side	Number of turns in coils	Wire diameter	Core Weight	Phase-configuration	Core material
	20	1.6 mm	4.81 kg	A, -C, B	Supermalloy

Table 3: Specifications for the road side coils and core in the basic solution used during the simulations.

Road side	Number of turns in coils	Wire diameter	Segment length	Phase-configuration	Core material
	20	1.6 mm	10 m	A, -C, B	Supermalloy

These configurations are chosen as the basis after early tests with core sizes, coil areas, conductor material and number of turns, but are together with current, frequency and air gap changed around these values in later simulations to determine their effects on the power transfer.

With the assumed segment length 44 coils per phase, 132 in total, are used over the 10 m length. This configuration leaves about 23 cm which are used to connect each segment to the grid.

4.2 Power transfer model

The FEMM-model used in the simulations is shown in Figure 27, with the transformer half in the road side continuing outside the bounding circle. This model is primarily used to obtain the self- and mutual-inductances and the magnetic flux density. The inductances are calculated by running a known current individually through each coil and in the program measuring the magnetic flux though every coil, including the one with the current in order to get the self-inductance, and then dividing the flux with the current. The inductances are then inserted into the previously mentioned inductance matrix to enable the current in the secondary side and the voltage in the primary side to be calculated in accordance with the three-phase version of equation (19).

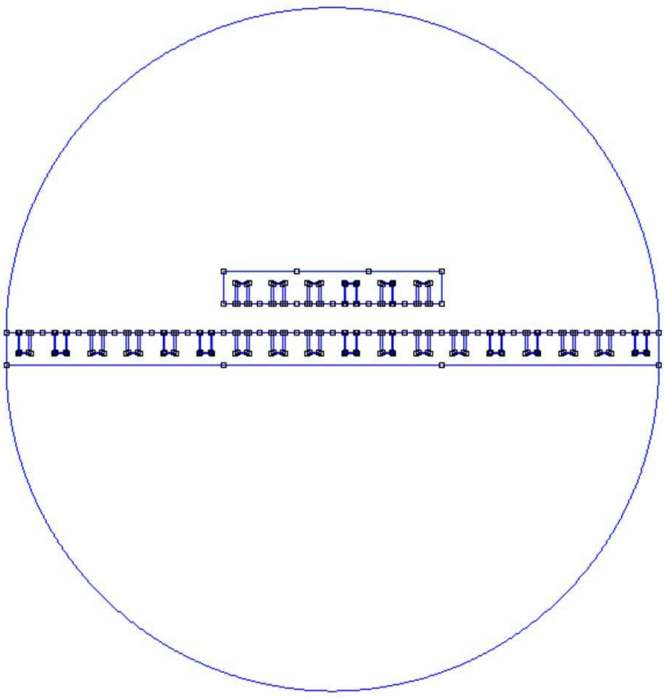

Figure 27: The FEMM-model used for the simulations.

4.3 Power loss model

As explained in chapter 2.6.1, using litz wire decrease the effect of both the skin effect and the proximity effect. For this reason and for simplicity's sake, the conductive losses are calculated using the DC-resistance for coil's wires, see equation (41).

In the case of the core losses where the equations are difficult to use, the shortcut described in chapter 2.6.1 is used to give approximate values for these. In Diagram 1 the loss curves for supermalloy at different frequencies are shown and from this the values for each frequency can be estimated (for a certain flux density level) and the result can be seen in Diagram 2.

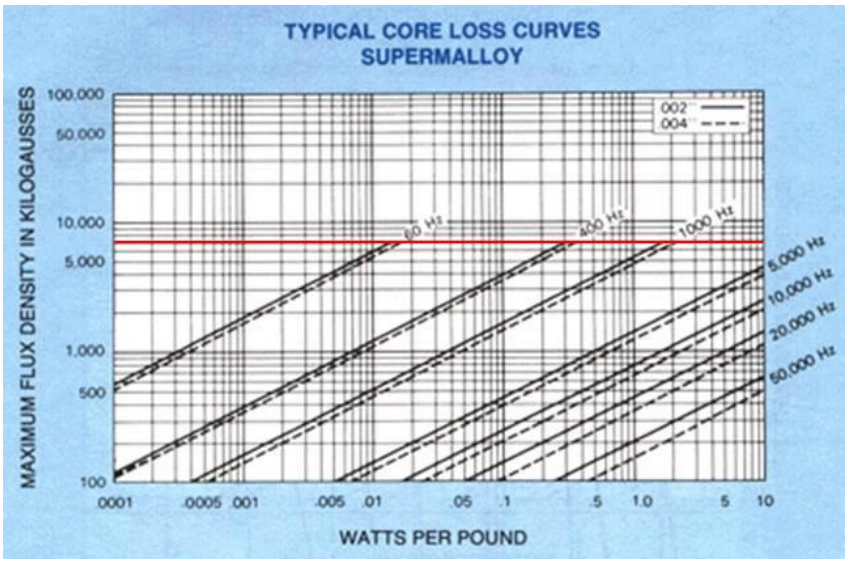

Diagram 1: Core losses for supermalloy at different frequencies with the approximate value for magnetic field density in the core shown as a red line[27].

[27] Magnetic Metals (2013) *Characteristics of Core Materials – Supermalloy*

The core losses for this diagram consist of both the hysteresis and the Eddy current losses.

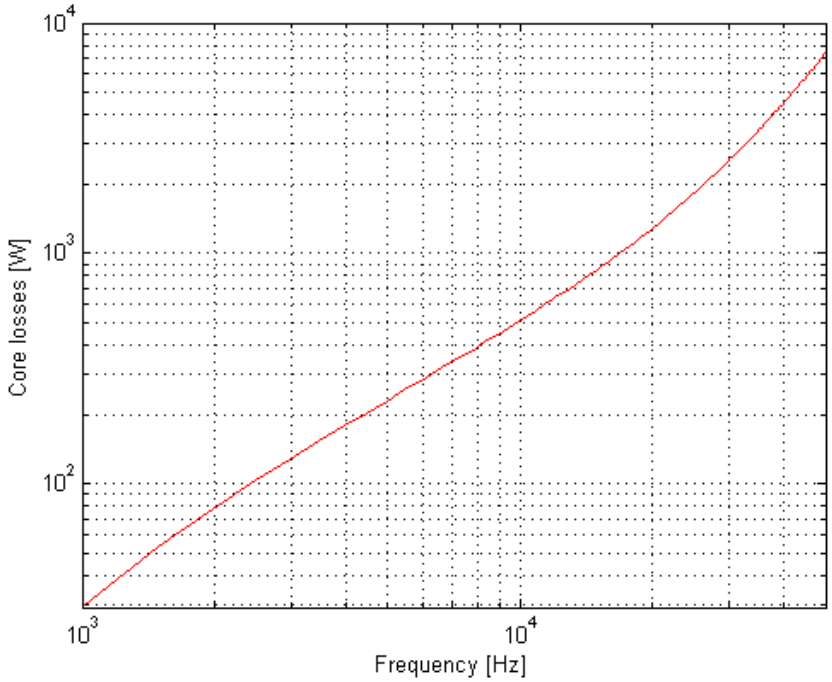

Diagram 2: Calculated loss curve for supermalloy at different frequencies for the proposed core.

The total losses are then calculated for a specific combination of frequency, current and size of coil and core.

4.4 System model

For a more detailed description of the different power electronic parts of the system, chapter 10.2 in the appendix may be read.

As stated in chapter 2.2, a high frequency is required to transfer enough power with a reasonable current. Since the frequency from the grid is either 50 or 60 Hz, depending on country, the current needs to go through a frequency changer. A method for doing so is to first rectify the current and then invert it back to AC with the desired frequency, known as an AC-DC-AC converter.

To avoid as much harmonic distortions as possible from the rectifier, a twelve-pulse bridge rectifier can be used instead. Because this rectifier results in 12-DC pulses per period instead of the normal six, the DC-voltage increases by a factor two, and the variations decreases.

The power inverter transforms the DC back to AC through switching, done with three transistor half-bridges. Each half-bridge is connected to one of the phases and since all transistors are controlled separately, a new three-phase system with a higher frequency than the source can be produced.

Even with the road side transformer half divided into segments, the losses would be too great if all coils within such a segment were conducting at the same time. In addition it would result in magnetic fields along the entire segment which could not be used since they would be too far away from the receiver under the vehicle. To avoid this and minimise the number of coils conducting at the same time, a system with each coil being controlled by a switch is proposed, see Figure 28. This way, only the coils which induce the most emf are used and the others are turned off, reducing the losses. As the vehicle moves along the road, the next coil starts conducting while the last is turned off.

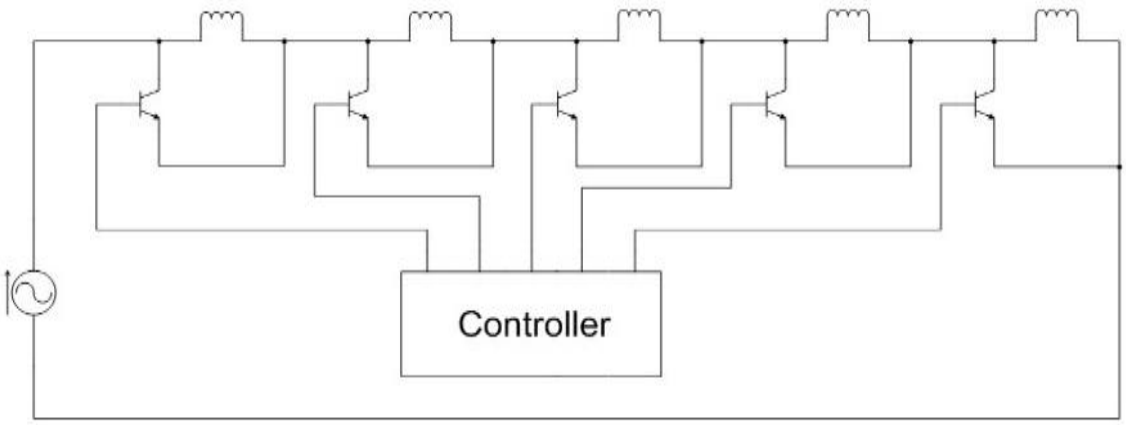

Figure 28: Principle for the control system.

For the controller to be able to know which coils should be on at a given time, the vehicle and road side must communicate with each other. A way to achieve this is to add a small antenna with focused transmission in the vehicle side and receivers in the road. This way, the road side controller can know exactly where the vehicle power receiver is in relation to the coils in the road and only turn on the ones closest to it.

5 Results

5.1 Power transfer capability

The objective was for a car to deliver 30 kW from the receiver which is 10 kW per phase. Simulations showed that because of the phase configuration in the receiver core, more emf was induced phase C than in the other two because it is placed in the middle of the core. For this reason the average power per phase was used as the criterion.

For the 200 kW a lorry needs either six or seven cores of the size used for a car. With six the total power sums up to 180 kW, and with seven it gives 210 kW. However if several of these cores are joined together to one or two longer, the end effect is reduced. This results in that the coupling factor becomes somewhat higher which means that a slightly power can be delivered from the receiver. This effect is already noticeable in the receiver in which phase C delivers a bit more power than phase A and B because it does not suffer from the edge effect. Although no tests regarding several of these cores joined together in the receiver side were made, using six cores result in more than 180 kW because of previously stated reason, which might be enough even though it is most likely less than the sought 200 kW.

For the determined distance between the primary and secondary side coils the current and frequency were changed to conform to the requirements. When the configuration was found, the air gap was varied to see how this affected the power and efficiency. A sensitivity study was also made in which additional design parameters were varied to determine how this affected the transfer.

Lastly, both the copper wires were exchanged with aluminium wires, but still assuming litz wires. This was done due to the fact that copper is more expensive than aluminium and therefore doing so might reduce the component cost but not the power losses. The current density for the different configurations which are discussed in this chapter is shown if Figure 29.

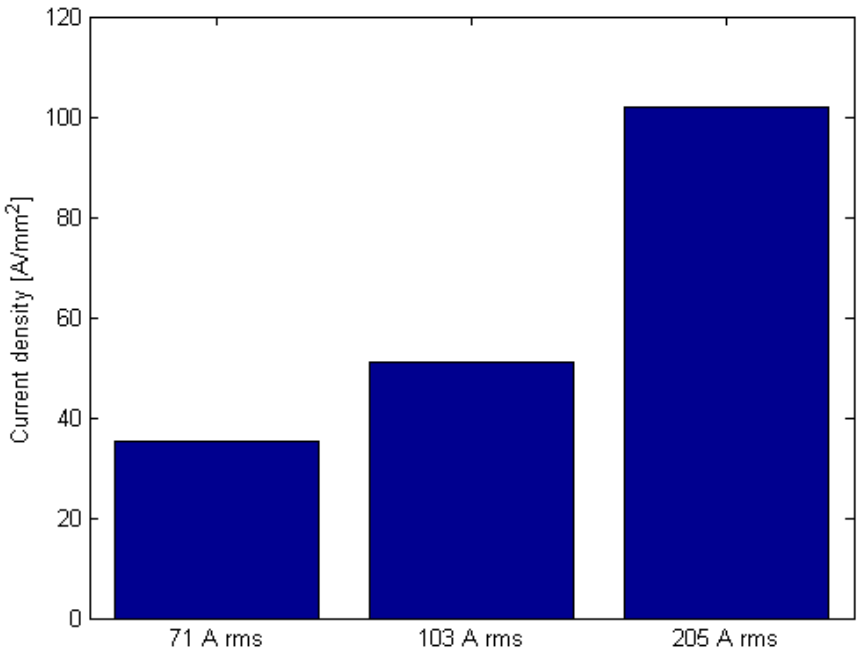

Figure 29: Current density in the wires for the three configurations.

The high value for conductor current density shown in Figure 29 indicates the lack of a thermal model in order to estimate the temperature rise in the components. As the main focus has been on the transferred power and the power output on the secondary side, the thermal issues related to high specific power losses has not been accounted when dimensioning the device. The power losses are accounted only in the efficiency calculations but not selecting the current level or size for the slots. Furthermore, the secondary load current is few degrees smaller than the magnetising current in the primary windings, which also caused the lack of concern towards the thermal issues. Therefore one of the limitations in this work has to be announced as a future work that is to choose the right dimensions for the windings and cores from thermal loading point of view.

5.1.1 Conventional road solution

With the conventional road design, meaning an air gap of 75 mm, and using copper wires, 10.6 kW rms per phase was achieved by running a current of 290 A peak (205 A rms) at 20 kHz. By varying the frequency of this current and the air gap, a power map which can be seen in Diagram 3 is made.

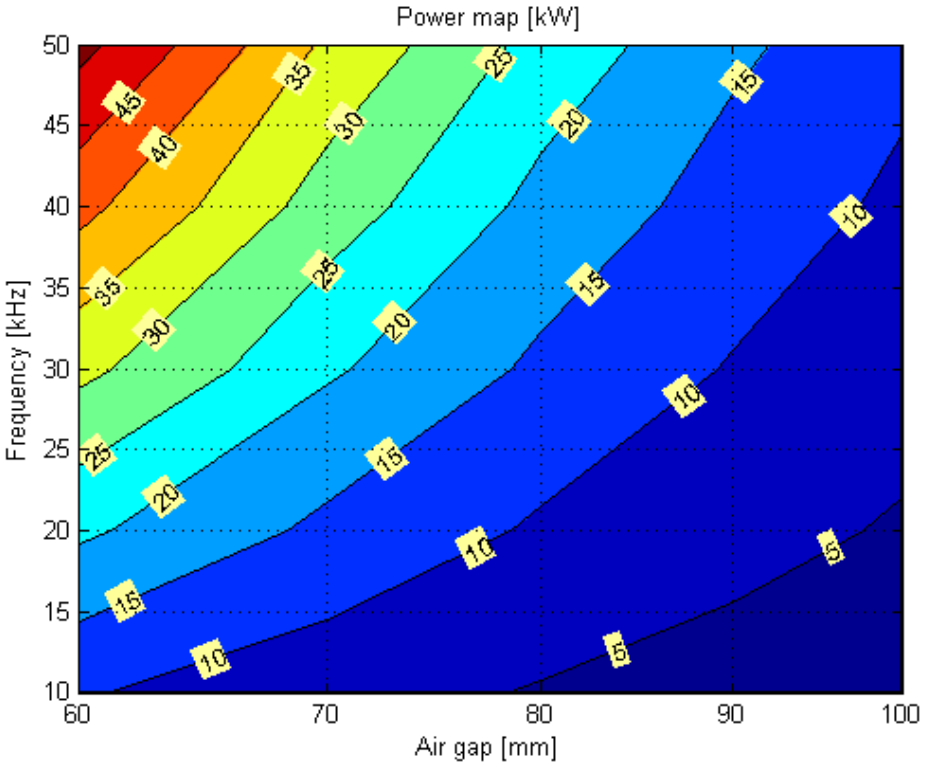

Diagram 3: Average transferred rms power per phase when running a peak current of 290 A at 20 kHz as reference point though copper wires. Note that the x-axis is in log-scale, but with linear labels.

When the copper wires are exchanged with aluminium wires and the same current as before is used, the power remains at 10.6 kW rms. By varying the same design parameters as before, a similar power map can be made and the result is shown in Diagram 4.

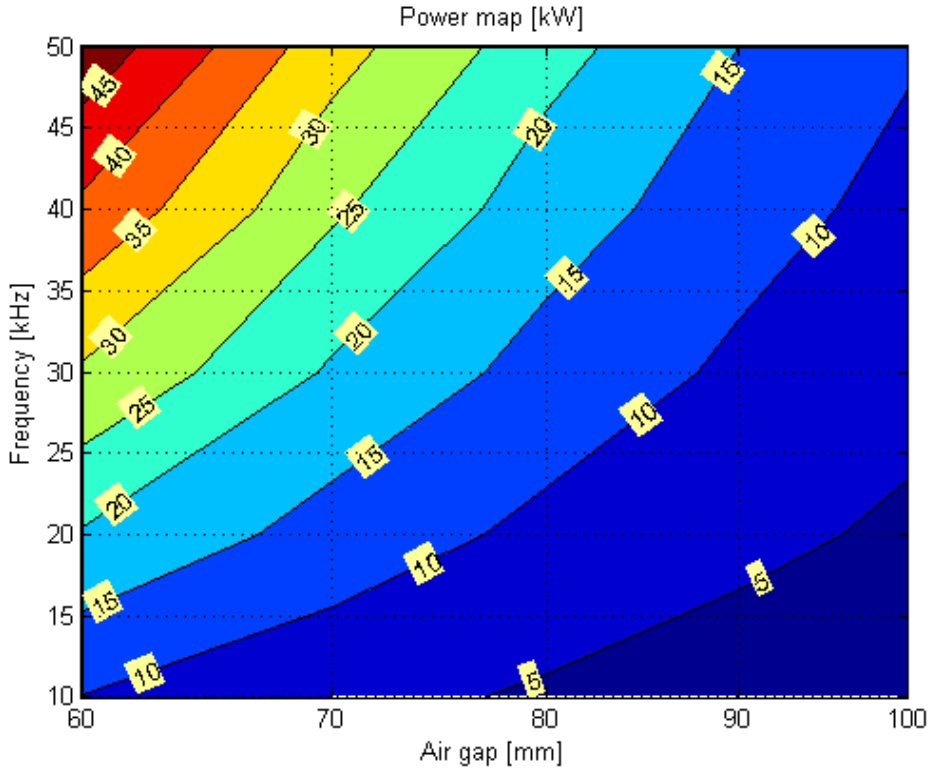

Diagram 4: Average transferred rms power per phase when running a peak current of 290 A at 20 kHz as reference point though aluminium wires. Note that the x-axis is in log-scale, but with linear labels.

5.1.2 Ideal road solution

Performing the simulations assuming the unconventional road solution previously described, the current can be decreased considerably. The tests showed that if the frequency was kept at 20 kHz, the current could be reduced to 100 A peak (71 A rms) and the power transferred would then be 10.1 kW rms. The power map from varying the distance and frequency with this configuration can be seen in Diagram 5.

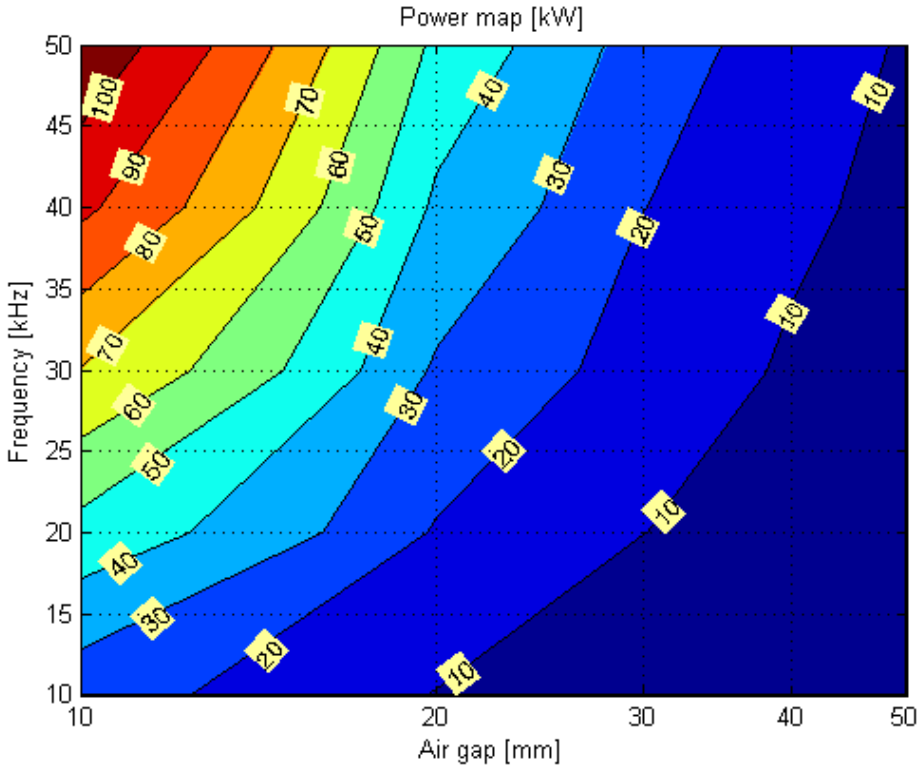

Diagram 5: Average transferred rms power per phase when running a peak current of 100 A at 20 kHz as reference point through copper wires. Note that the x-axis is in log-scale, but with linear labels.

At this air gap, tests with the frequency 10 kHz were also performed, and 10.6 kW rms could be transferred with the current 145 A peak (103 A rms). The results from these are shown in the power map in Diagram 6.

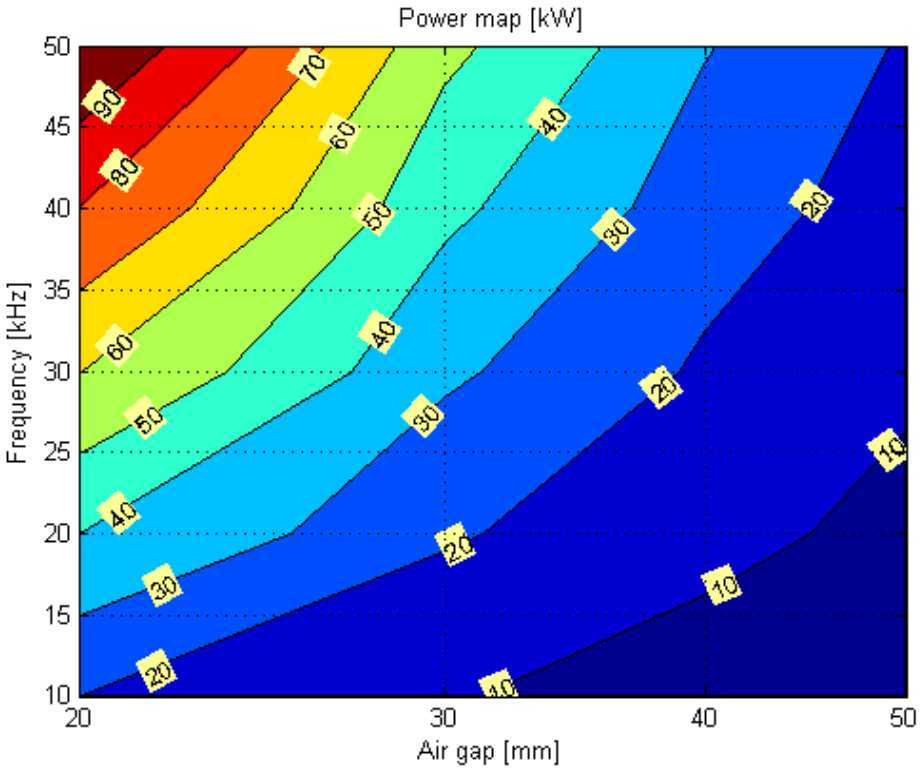

Diagram 6: Average transferred rms power per phase when running a peak current of 145 A at 10 kHz as reference point through copper wires. Note that the x-axis is in log-scale, but with linear labels.

Exchanging the copper wires for aluminium wires with the 30 mm air gap does not require any change in either current of frequency. 10.1 kW rms can be transferred using a current of 100 A peak at 20 kHz. The results are shown in Diagram 7.

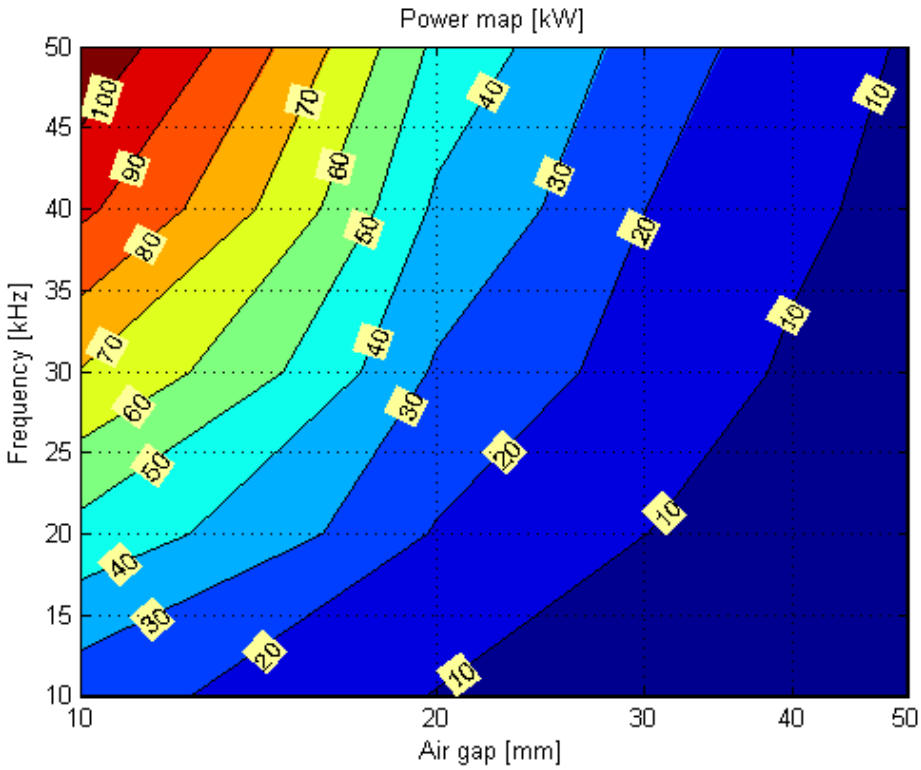

Diagram 7: Average transferred rms power per phase when running a peak current of 100 A at 20 kHz as reference point though aluminium wires. Note that the x-axis is in log-scale, but with linear labels.

The same is true when the frequency is changed to 10 kHz; a 145 A peak current gives 10.6 kW rms, and the result is shown in Diagram 8.

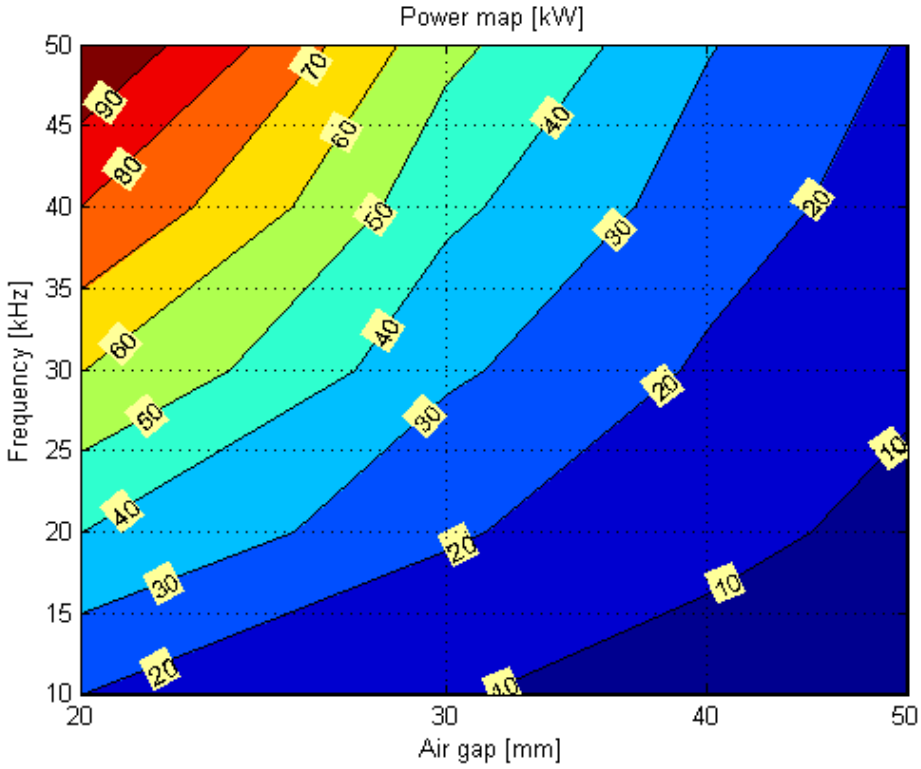

Diagram 8: Average transferred rms power per phase when running a peak current of 145 A at 10 kHz as reference point through aluminium wires. Note that the x-axis is in log-scale, but with linear labels.

5.2 Power transfer efficiency

With the power loss model specified in chapter 4.2 the efficiency can be calculated and depends on the current and the wire material (conductive losses), and the frequency and core material (core losses). The efficiency is calculated for the active power transfer in the partially coupled transformer, so losses in the power electronics are excluded since a detailed choice regarding these are not a part of this thesis.

5.2.1 Conventional road solution

For the 75 mm air gap 290 A peak was needed at 20 kHz to achieve the desired 10 kW power transfer. Adding the losses and to the calculations resulted in the efficiency 70.6 %. Varying the frequency and the distance in the same way done when looking at the power, an efficiency map is made and for this configuration is shown in Diagram 9.

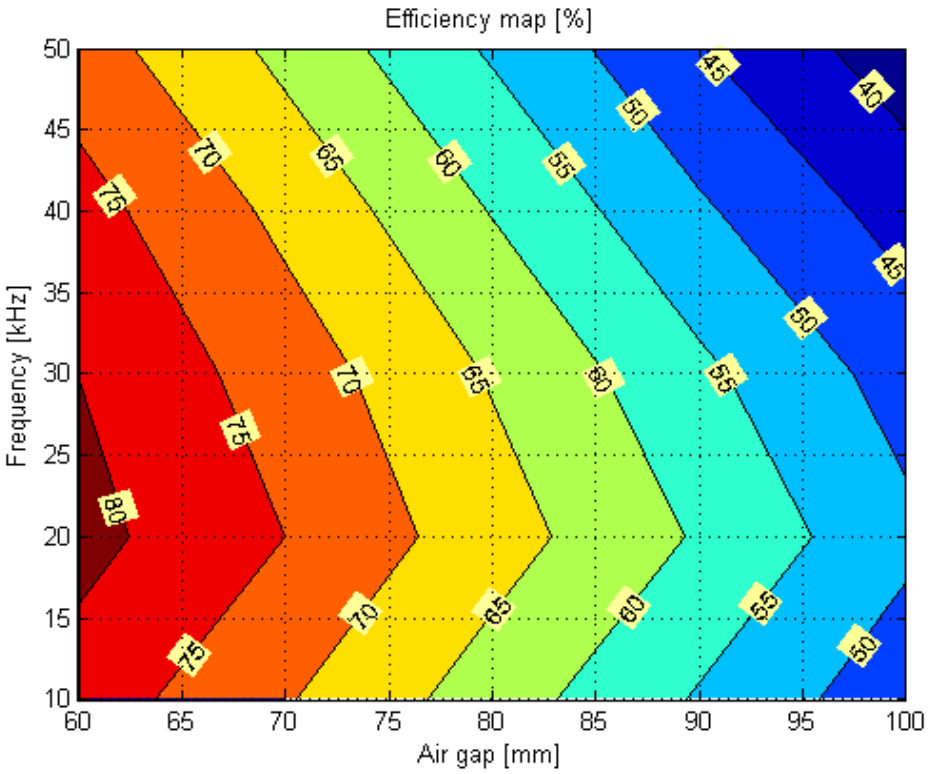

Diagram 9: Average efficiency of the wirelessly transferred power when running a peak current of 290 A at 20 kHz as reference point through copper wires.

For the aluminium wires the efficiency decreases to 66.1 % and the power map is shown in Diagram 10.

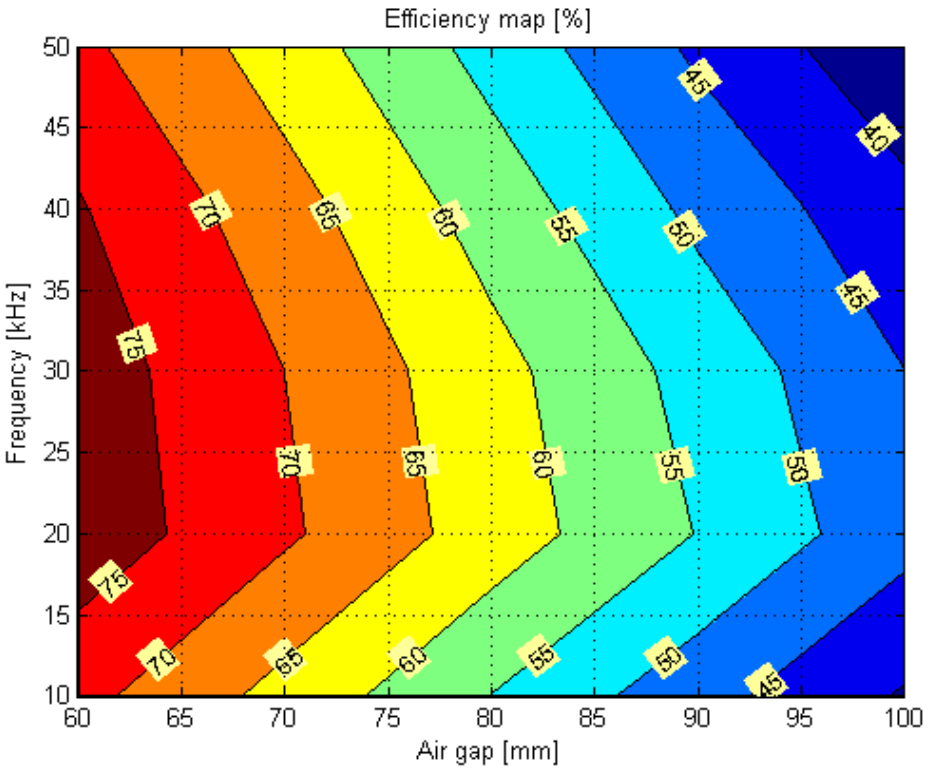

Diagram 10: Average efficiency of the wirelessly transferred power when running a peak current of 290 A at 20 kHz as reference point through aluminium wires.

5.2.2 Ideal road solution

For the first configuration with the 30 mm air gap and running a current at 20 kHz, the efficiency becomes 76.6 %. The power map with these parameters chosen can be seen in Diagram 11.

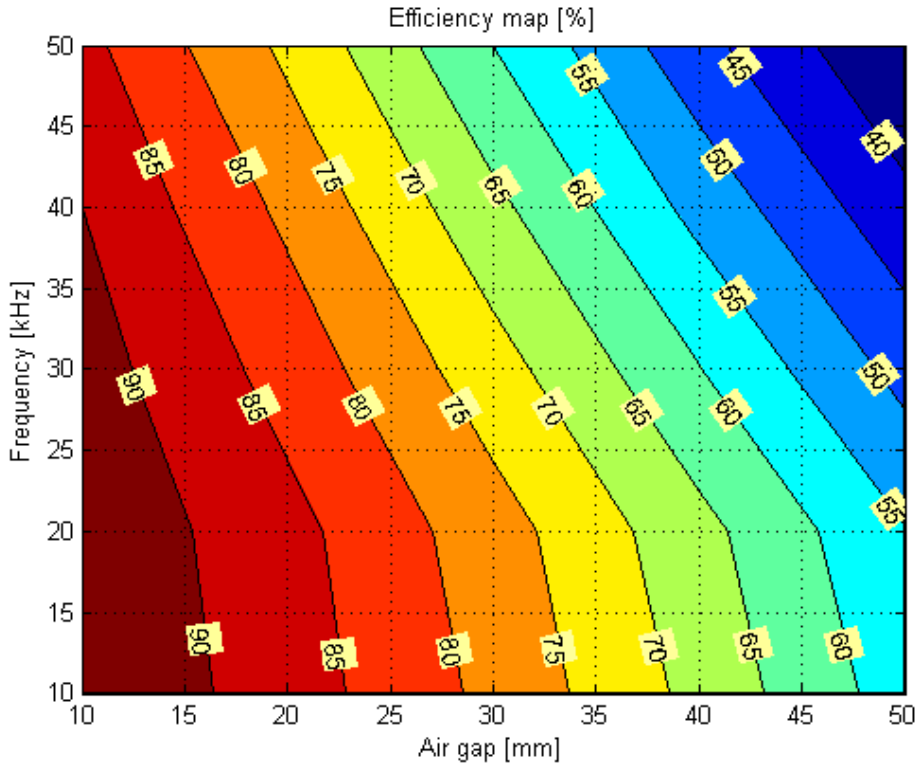

Diagram 11: Average efficiency of the wirelessly transferred power when running a peak current of 100 A at 20 kHz as reference point through copper wires.

Keeping the air gap at 30 mm while reducing the frequency to 10 kHz, and increasing the current to 145 A peak results in an efficiency of 86.9 %, and the map is seen in Diagram 12.

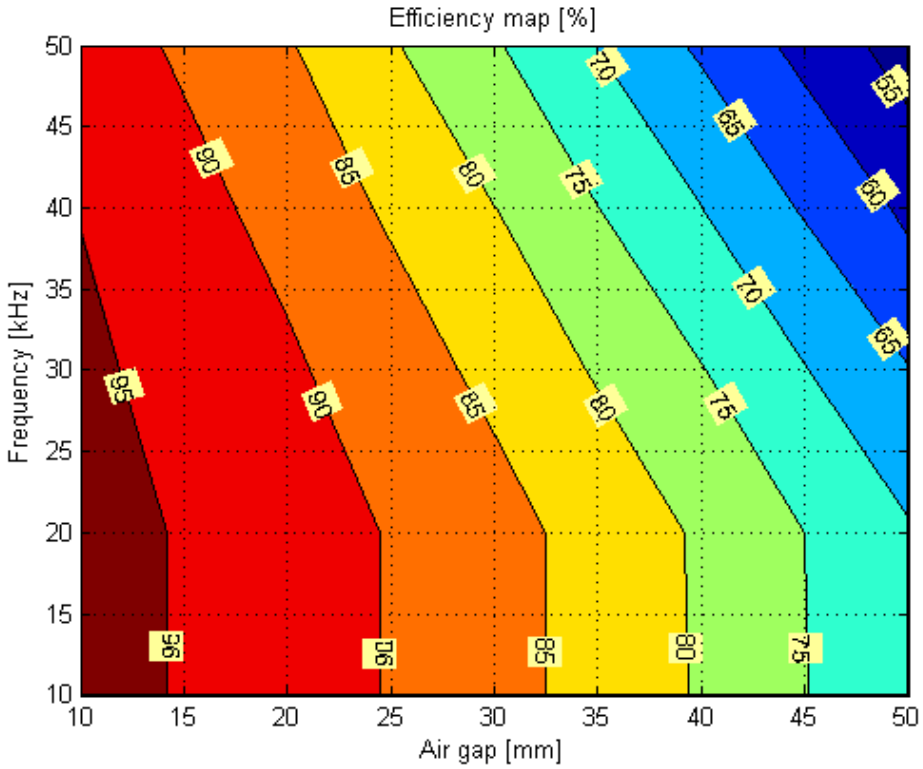

Diagram 12: Average efficiency of the wirelessly transferred power when running a peak current of 145 A at 10 kHz as reference point through copper wires.

When using the 20 kHz configuration with aluminium wire, the efficiency becomes 75.8 % and the results are shown in Diagram 13.

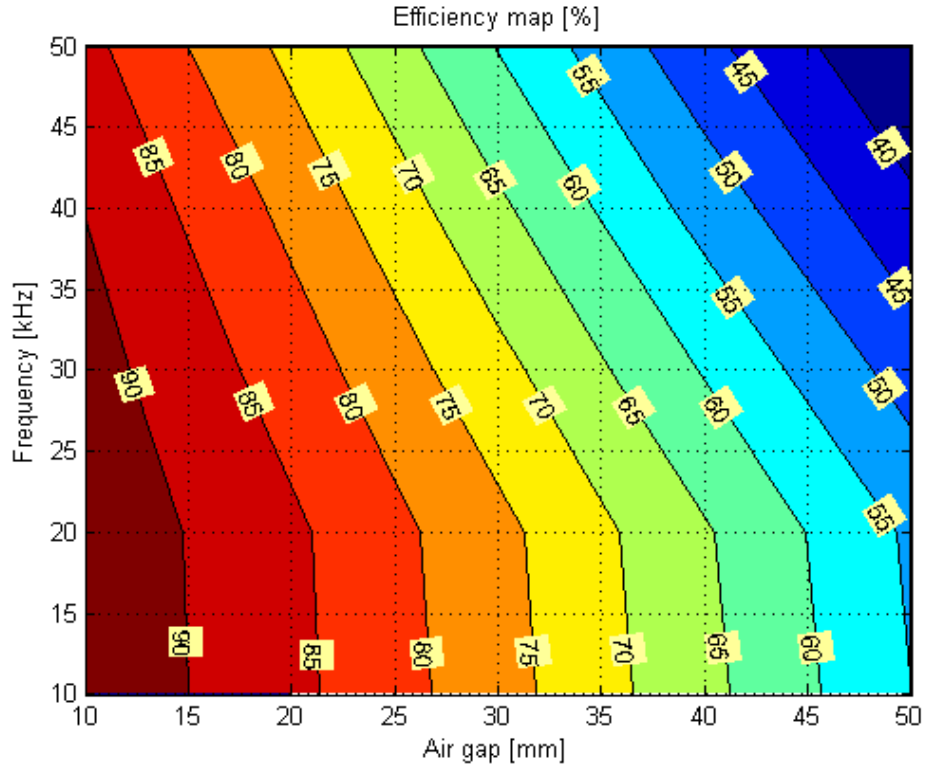

Diagram 13: Average efficiency of the wirelessly transferred power when running a peak current of 100 A at 20 kHz as reference point through aluminium wires.

Decreasing the frequency to 10 kHz and increasing the current to 145 A results in an efficiency of 84.7 %. These results are shown in Diagram 14.

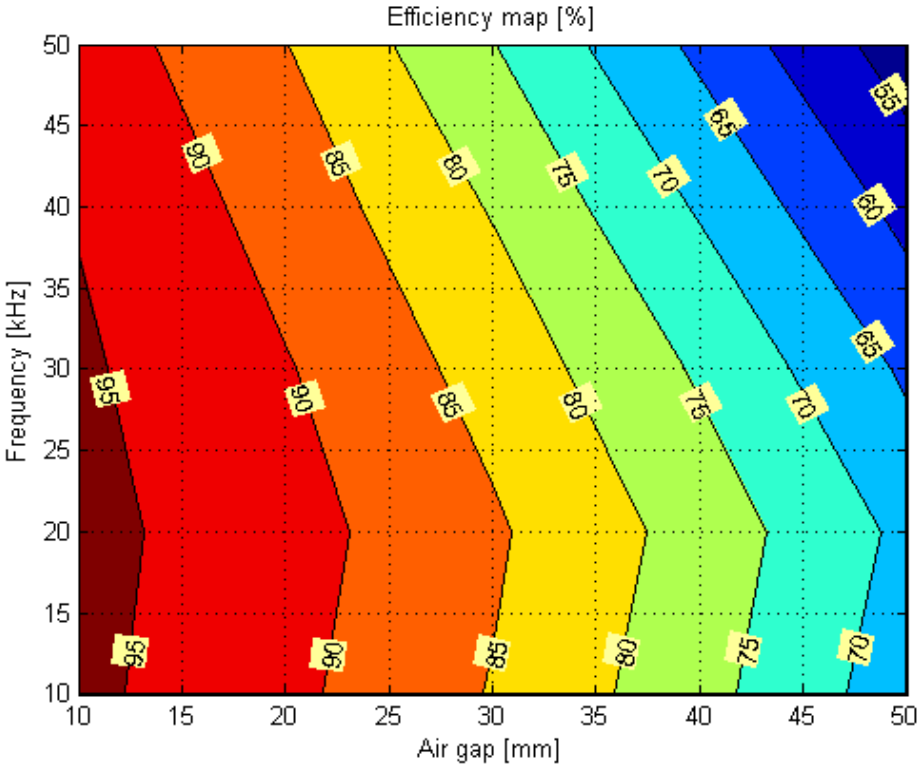

Diagram 14: Average efficiency of the wirelessly transferred power when running a peak current of 145 A at 10 kHz as reference point through aluminium wires.

5.3 Scalability

By varying different design parameters, it becomes possible to see how sensitive the system is for changes occurring from the power supply (current and frequency variations) and vertical movement of the receiver. It is also possible to see how changing certain specifications when building the system can affect the outcome. Although more core materials than supermalloy was tested, only the results for this are included since it is the only one that losses were found for.

These simulations were only made with copper wires since the difference between the two conductor materials was only noticeable with the efficiency, and the difference was small.

5.3.1 Traditional road solution

For the 75 mm air gap the result from the sensitivity analysis regarding the power transfer can be seen in Table 4, and in Table 5 the result regarding the efficiency is shown.

Table 4: Sensitivity analysis of transferred power in one phase for different changes of design parameters (0% translates to 10.6 kW rms).

Design parameters		Change of parameters vs. delivered power				
		-20%	-10%	0%	+10%	+20%
Dimension parameters	Air gap	+84.9%	+34.9%	0%	-25.0%	-42.9%
	Number of turns in coils	-35.9%	-19.0%	0%	+20.8%	+43.4%
	Coil area	-20.1%	-10.1%	0%	+10.4%	+19.8%
Electrical parameters	Current	-35.9%	-19.0%	0%	+20.8%	+43.4%
	Frequency	-20.0%	-10.0%	0%	+10.4%	+19.8%

Table 5: Sensitivity analysis of transfer efficiency for different changes of design parameters.

Design parameters		Change of parameters vs. efficiency				
		-20%	-10%	0%	+10%	+20%
Dimension parameters	Air gap	81.2%	76.3%	70.6%	64.8%	58.9%
	Number of turns in coils	63.8%	67.6%	70.6%	73.0%	75.0%
	Coil area	68.9%	70.0%	70.6%	71.3%	71.8%
Electrical parameters	Current	63.8%	67.6%	70.6%	73.0%	75.0%
	Frequency	70.1%	70.6%	70.6%	70.5%	70.3%

5.3.2 Ideal road solution

For the 30 mm air gap the results from the sensitivity analysis for the power transfer and efficiency using the 145 A and 10 kHz configuration are shown in Table 6 and table Table 7.

Table 6: Sensitivity analysis of transferred power in one phase for different changes of design parameters (0% translates to 10.6 kW rms).

Design parameters		Change of parameters vs. delivered power				
		-20%	-10%	0%	+10%	+20%
Dimension parameters	Air gap	+44.3%	+19.8%	0%	-15.6%	-28.3%
	Number of turns in coils	-36.0%	-19.1%	0%	+20.8%	+44.3%
	Coil area	-20.1%	-10.0%	0%	+10.4%	+19.8%
Electrical parameters	Current	-36.0%	-19.1%	0%	+20.8%	+44.3%
	Frequency	-24.1%	-10.2%	0%	+10.4%	+19.8%

Table 7: Sensitivity analysis of transfer efficiency for different changes of design parameters.

Design parameters		Change of parameters vs. efficiency				
		-20%	-10%	0%	+10%	+20%
Dimension parameters	Air gap	90.5%	88.7%	86.9%	84.9%	82.7%
	Number of turns in coils	82.5%	85.0%	86.9%	88.3%	89.4%
	Coil area	86.1%	86.5%	86.9%	87.2%	87.4%
Electrical parameters	Current	82.5%	85.0%	86.9%	88.3%	89.4%
	Frequency	85.9%	86.6%	86.9%	87.0%	87.1%

5.4 Hovering

Using the method described in chapter 2.4.1.1, the requirement for achieving the lift with the hovercraft technique can be calculated. Starting with using only the weight of the core of the receiver (4.8 kg) as the mass in the equation and assuming the length and width of the receiver's base to be 250 and 200 mm respectively, the pressure and air flow can be calculated for a hovering height set to be 10 mm.

The pressure inside the skirt becomes about 1200 Pa and the air flow from it becomes almost 190 litres of air per second.

By doubling both the length and the width of the receiver, the pressure is decreased to just over 300 Pa. The air flow however remains the same as before.

Further iterations of the calculations show that as long as the factors used to change the length and width are the same, the air flow does not change. The pressure inside the skirt decreases roughly with the area of the receiver cubed.

As for the rigid and complaint air bearing systems, no real calculations were able to be made. However both systems have a very high lift capacity and need much less air than a hovercraft solution does. The only real problem is with the road, which needs to be fairly smooth, especially for the rigid air bearing system.

Tests were also made regarding magnetic levitation but for this to be an option the distance between the coils in the road and receiver side could not be more than 10 to 15 mm. At 30 mm the repelling force was already so weak that it made no real difference.

During the magnetic hovering tests, lateral positioning through magnetic force was also tested. Instead of having just one row of coils in the road, two would be used with spacing in between so that the receiver would lay stable there, see figure xx. Before any results were able to be obtained the idea proved to be impractical since the magnetic flux through the vehicle side coils decreased several hundred times compared to when only one row was used. This means that it would severely decrease the power transfer and efficiency since a higher current would have to be used and with more core material, hysteresis and Eddy current losses would double.

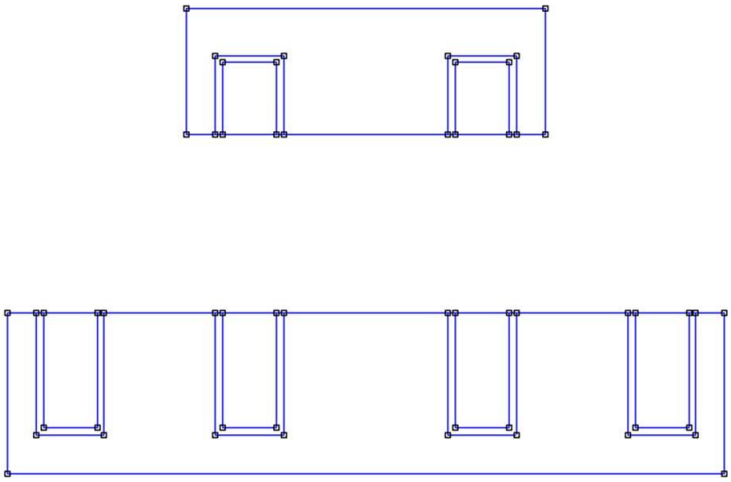

Figure 30: Configuration for lateral positioning with the coils going into the picture, as seen before.

5.5 Shielding

Measuring the magnetic field density at different distances from the road side coils shows why shielding is necessary. The magnetic field density measured from the FEMM-simulations for the 100 A at 20 kHz configuration is plotted in Diagram 15 and Diagram 16.

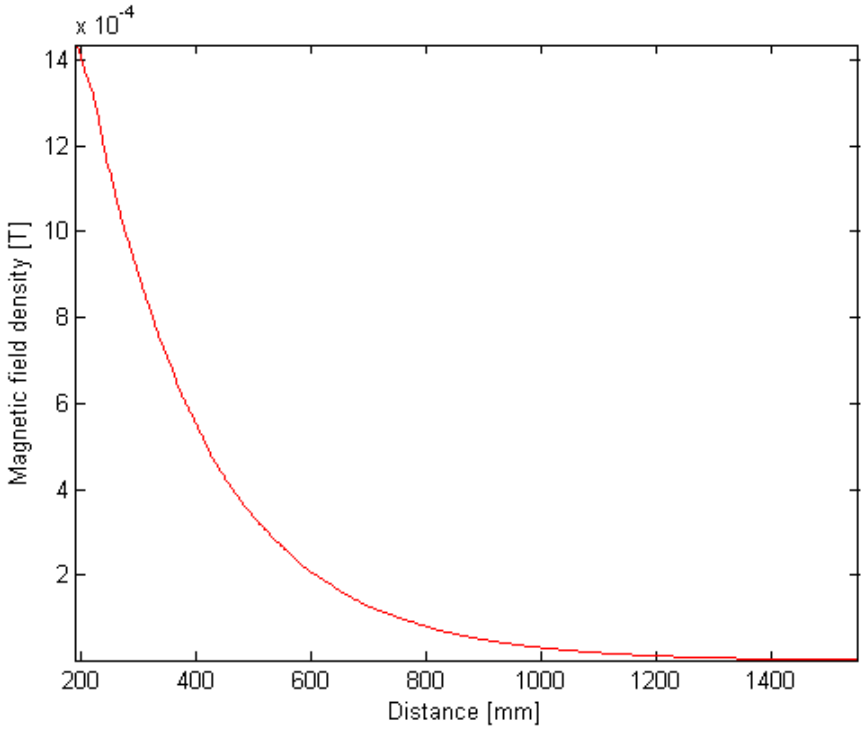

Diagram 15: Magnetic field density from the road side coil at increasing distances.

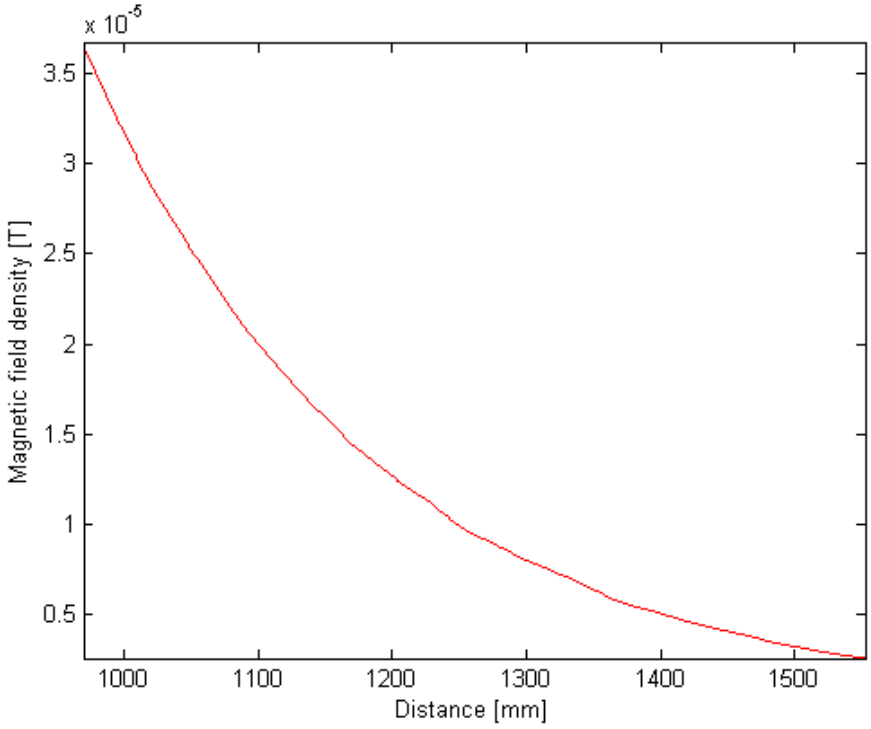

Diagram 16: Zoomed in view of the magnetic field density from the road side coil at increasing distances.

When 100 A is run through the coils in the road side, the magnetic field density still has a value of about 30 µT one meter from the coils. It takes an additional 30 to 40 cm before the density is within the set limit. For the 290 A solution, the limit is not met until about 1.6 m from the coils.

6 Analysis

What the results foremost show is that achieving the desired power transfer is most definitely possible. By decreasing the air gap the amount of core material, wires and power needed can be drastically lowered and thereby making a system covering all the major freeways more economically feasible than if the existing solutions were used.

Depending on the distance a current between 100 and 300 A peak is needed, and the system is most efficient when the frequency is 10 to 20 kHz. Lowering the frequency further makes the power transfer more difficult since a higher current must be used. It still shows that it can be done with a reasonable efficiency, even for the worst case scenario tested with the 75 mm air gap and aluminium wires. Although the conductive losses were estimated with the DC resistance in the simulations, the AC resistance demands that a wire is chosen which minimises these losses, such as litz wires.

In accordance with the physics of electromagnetism, the number of turns in the coils has about the same effect on the transferred power as the current. This means that these two design parameters are easy to compensate for if one is changed when the system is being built. Changing the material of the wires between copper and aluminium has close to no impact on the transferred power, but the efficiency goes slightly down when latter is chosen. As copper is more expensive, a compromise has to be made between construction cost and efficiency when this design parameter is chosen for a realisation.

Although the cross sectional area of the coils have a relative low impact on the transferred power and the efficiency compared to some of the other parameters, it is one of the most important since over 20 tonnes of the chosen material is needed per km road. In addition to this, almost 5 kg are needed per car and almost 29 kg for a lorry. From this it becomes clear that even more work is needed to minimise the size of the cores. This will then need to be compensated, for instance by increasing the current. As for the core material itself; it needs to have a high enough magnetic saturation for it to be able to support the magnetic field induced by the current. It is also important that it can be used for high frequency applications without the losses becoming too large. To minimise the core losses it has to be built either with laminates or powder, which reduces the area over which Eddy currents can pass. It also needs to be a soft magnetic material to reduce the hysteresis losses. Due to hardship with finding data for material losses, only supermalloy was tested in the final configuration. In the beginning of the testing when only the power transfer and not the efficiency was in focus, iron was used because of its great magnetic properties. However later simulations showed that supermalloy worked almost as well for transferring power making it a fine choice from the technical perspective.

For the car configuration the results show that the necessary power can be the transferred with a high efficiency for both the 75 mm and the 30 mm air gap. The key is as suspected from the beginning, to minimise the air gap, which is accomplished with air bearing, to achieve maximum efficiency with minimum effort and cost. Using the complaint, or with unconventional road construction, rigid air bearing system should make this possible at the very least in theory. Developing a design specified for this application is needed to truly ascertain how well it would work in reality, but the using the technique is promising and a determining factor for the system proposed in the report to ever becoming a reality.

As for the case with the lorry, the results show that if six cores are used but are not connected, and have their own air bearing systems and regulators, the transferred power sums up to 190.8 kW. This shows that if two or three core segments are joined together and the new and bigger segments have their own air bearing systems and regulators facilitating the positioning over the whole length, 200 kW transferred might be possible, or at least nearly possible. If the cores are divided into two groups instead of just one, the regulation becomes easier since the new cores are shorter and therefore it becomes less problematic keeping the whole length over the coils in the road and on the excitation track. To guarantee at least 200 kW, seven segments have to be used. This brings the total power to 222.6 kW, but as seven is not evenly dividable, the joined segments will be different in size. This means that different sizes of air bearing systems must be used which might make production more complicated. The actual power transferred and required needs to be determined in more detail to specify how the solution for lorries should be.

Combining or even substituting the air bearing system with magnetic levitation showed to not be possible. Because all surrounding conducting coils affect the amplitude of the emf and its phase in a coil, the current through it induces a magnetic field which is not directly opposite that of the coil right below. This decreases the force repelling the two sides, and simulations show that in order for the force to be large enough to substitute the air bearing system, the air gap can only be around 10 to 15 mm. This leaves very little space for covers in both the road side and on the vehicle side, and for variations in the air gap caused by minor oscillations when driving.

When it comes to shielding form the magnetic field from the system, the people inside the vehicles do not have to worry since the metal chassis of the vehicles works well for this. For the field leaving the volume under the car to the sides, there might be a need for shielding. As discussed in the results it takes about 1.6 m before the field density is at the same level as the limit when running a 290 A current. This means that it could be a problem for passing vehicles if the doors do not block enough of the field, but also for workers during road work and police officers and ambulance nurses which can also be present on the side of and on the roads. Active shielding might be problematic due the three-phase system used so a passive shield is most likely the best option. A way to do this is by having metal plates buried on either side of the coils, and having metal brushes form the car be in contact while driving. These will have to be fastened to the rest of the system since they also require the same regulation as the power receiver to maintain the contact with the ground shields.

7 Design examples

From the analysis two designs are proposed, one for the traditional road configuration, and one for the imagined unconventional road solutions. The options are made to present maximum performance, with no regards to which would be the best from an economical point of view. The two solutions are the same on several design parameters, and these are reviewed first.

The unit on the vehicle side is suspended by an arm which can raise and lower it, and also move it sideways to keep the receiver over the track in the road. To keep track of how to regulate, the receiver needs magnetic field sensors on both side of the core to measure the difference in the field. At least two sensors on each side are needed, both for accuracy and redundancy.

The core in the vehicle side is, as previously stated, composed of laminates made out of supermalloy. The basic shape is a block 100 mm wide, 222 mm long and 33 mm thick. The teeth are 27 mm long, except the two outer ones which are 13.5 mm long. The slots in which the coils are placed are 10 mm wide and 20 mm deep. This is shown graphically in Figure 31.

For the lorry solution, six core segments are used and joined together into two 666 mm long segments and they each have their own air bearing system and regulator. This means that the size of the air bearing systems have to be about 700 to 750 mm across.

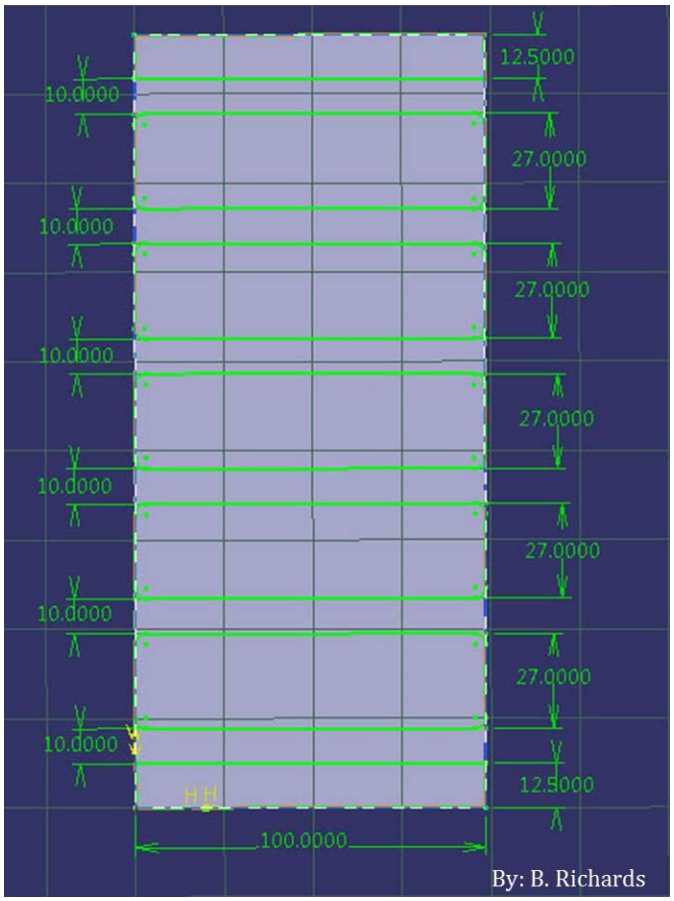

Figure 31: View of the vehicle side core (see **Figure 6**) from the above with the dimensions marked (note that the figure says 12.5 at the end, which should be 13.5).

The wires used are Litz wires, which are made from copper and have a diameter of 1.6 mm. The coil consists of 20 turns bringing the fill factor to circa 60% and the size of the coils is 100 times 100 mm. The coils are configured in the following order: A, -C, B, -A, C and –B.

The same cores as in the vehicles are used in the road, but placed in a long row. The road is divided into segments 10 m of length; each containing 44 individual cores. This leaves an additional 23 cm for connection to the grid.

Each individual coil in every phase in a segment can be turned on or off individually by a switch which is controlled by a signal from an antenna in the receiver. This antenna also sends the car's information so that the correct person can be charged for the electricity.

From the supply the power goes through a frequency changer, consisting of a 12-pulse rectifier, a DC-link and a power inverter before reaching the coils.

7.1 Conventional road solution

As determined by the results in chapter 5, the amplitude and frequency of the current needed is 290 A peak and 20 kHz.

When it comes to the air bearing system for this configuration, the complaint air bearing system described in chapter 2.4.1.3 is used. It can handle variations of a few centimetres in the road and the air requirements are relative low. The smallest sizes these already come in are 254 mm (10 inches)

across, which works well with the length of the core, which is 222 mm. This also leaves room for the air tubes, sensors and antenna on both the sides of the core, which is only 100 mm wide.

If the asphalt in the wearing course cannot be made smooth enough for the air bearing to work, it would be possible to substitute it for concrete over the part of the road where the coils are placed.

7.2 Ideal road solution

When imagining a road solution making it possible for the air gap to be reduced to 30 mm, the most efficient current and frequency configuration is 145 A peak at 10 kHz, as determined by the results in chapter 5. Using the lower frequency option here is better because the core losses decrease more than the conductive losses increase due to the larger currents in the coils.

Using titanium as described previously as cover for the coils in the road and as surface for the air bearing system means that the surface is smooth enough for the rigid air bearing system to be used, which was described in chapter 2.4.1.2. This enables the coils to be closer while power is transferred which minimises the losses caused by distance.

8 Conclusion

The goal of this master thesis regarding inductive energy transfer for vehicular applications is to transfer 30 and 200 kW to light and heavy vehicles respectively. With traditional and unconventional road design, a magnetic air gap of 75 and 30 mm respectively is estimated. Based on these assumptions and the proposed large air gap three-phase transformer, this work shows that a 290 A peak current at 20 kHz, through a single core unit, delivers roughly 30 kW for light vehicles with an efficiency of 70.6 %. Combining six of these core units into two (or possibly three) longer units will transfer enough power for heavy vehicles. In Figure 32 the system under a bus is illustrated to give a clearer sense of the size.

Figure 32: Size of the system compared to a bus.

For the 30 mm estimation the works shows that a 140 A peak current at 10 kHz delivers the required 30 kW for light vehicles, but at an efficiency of 86.9 %. As with the 75 mm magnetic air gap, six single core units are combined to deliver the required power for heavy vehicles.

The final thoughts regarding this project can be started with the fact that the produced results which are presented here supports the idea by Bryan Richards, that air bearing can be used to improve already existing solutions for inductive power transfer for electric vehicles. The power needed is decreased and the size and cost of coils and cores are minimised as a result of bringing the two transformer halves closer with air bearing.

However this statement only takes into account the technical aspects, mainly revolving the actual power transfer, but the economic factors cannot be overlooked. In future projects it needs to have a more central role as it will be a, if not the, determining factor for some choices such as core and wire material.

There is more work that needs to be done regarding the technical aspects too. The two most important of these are core material and air bearing. For the possible core materials a deeper study of the losses they suffer due to high frequencies needs to be done. The amount of magnetic field density which can flow though it before it gets saturates is also an important factor since this helps determining how much thinner the core can be made to reduce weight and cost.

For the air bearing solution a model specified for the application must be made and tested to see how it performs under the circumstances determined in this report. The results regarding the solution presented here are based on the general guidelines available and estimations from offered data. Determining factors are what surfaces it can handle, the air flow needed to sustain the hovering, and by extension the power needed to supply the system with said air. Wear and tear of the diaphragm material needs to be tested if the complaint air bearing system is chosen.

Other aspects which need further research are the determining the power electronics, resonance compensation, regulation of the receiver and communication with the road to determine which coils should be on and off, and when to turn them on and off respectively and this communication can incorporate vehicle information for billing.

The most important aspect regardless of what way is chosen for electric vehicles, is that the electricity which is used to supply them must be from sustainable sources. Otherwise gasoline might as well be fabricated from coal as it will be just as bad for the environment.

9 References

[1] I.D. Mayergoyz, W. Lawson. *Basic Electric Circuit Theory*. Academic press, London, 1996.

[2] Wikipedia contributors. Flexible AC transmission system [Internet]. Wikipedia, The Free Encyclopedia; 2013 Apr 5, 04:53 UTC [cited 2013 May 18]. Available from: http://en.wikipedia.org/w/index.php?title=Flexible_AC_transmission_system&oldid=548783590.

[3] CUA (2008) [Online] [cited 2013 April 14]. Available from: http://students.cua.edu/51mcmahon/Lift_System/calculations/lift_calculations.pdf

[4] J. Perozzo. *Hovercrafting as a Hobby*. Maverick Publications, Bend, 1995, p. 27.

[5] Airfloat (2012 May) *How Air Bearing Works* [Online] [cited 2013 May 17]. Available from: http://www.airfloat.com/airfloat/wp-content/uploads/2012/05/How-Air-Bearings-Work.pdf

[6] Airfloat (2013 January) *Minimum Estimated Air Consumption for Air Bearings* [Online] [cited 2013 May 21]. Available from: http://www.airfloat.com/airfloat/wp-content/uploads/2013/01/calc_air_consump_b.pdf

[7] F.P. Gram (2003, January 23) *Magnetic Field and Forces* [Online] [cited 2013 April 3]. Available from: http://instruct.tri-c.edu/fgram/web/Mdipole.htm

[8] Wikipedia contributors. Electromagnet [Internet]. Wikipedia, The Free Encyclopedia; 2013 May 3, 00:08 UTC [cited 2013 April 3]. Available from: http://en.wikipedia.org/w/index.php?title=Electromagnet&oldid=553274838.

[9] Vågbrytaren Stockholm (2012, February 9) *Gränsvärden för elektriska och magnetiska fält samt elektromagnetiska vågor – strålning* [Online] [cited 2013 May 20]. Available from: http://www.vagbrytarenstockholm.se/gransvarden

[10] Wikipedia contributors. Earth's magnetic field [Internet]. Wikipedia, The Free Encyclopedia; 2013 May 21, 14:45 UTC [cited 2013 May 22]. Available from: http://en.wikipedia.org/w/index.php?title=Earth%27s_magnetic_field&oldid=556112212.

[11] Wikipedia contributors. Electromagnetic shielding [Internet]. Wikipedia, The Free Encyclopedia; 2013 May 20, 10:26 UTC [cited 2013 May 22]. Available from: http://en.wikipedia.org/w/index.php?title=Electromagnetic_shielding&oldid=555925442.

[12] Wikipedia contributors. Copper [Internet]. Wikipedia, The Free Encyclopedia; 2013 May 23, 21:40 UTC [cited 2013 April 6]. Available from: http://en.wikipedia.org/w/index.php?title=Copper&oldid=556489420.

[13] Wikipedia contributors. Aluminum [Internet]. Wikipedia, The Free Encyclopedia; 2013 May 18, 00:42 UTC [cited 2013 April 6]. Available from:

http://en.wikipedia.org/w/index.php?title=Aluminium&oldid=555588706.

[14] Wikipedia contributors. Electrical resistivity and conductivity [Internet]. Wikipedia, The Free Encyclopedia; 2013 May 9, 02:40 UTC [cited 2013 April 10]. Available from: http://en.wikipedia.org/w/index.php?title=Electrical_resistivity_and_conductivity&oldid=554227622.

[15] N. Mohan, T. Undeland, W. Robbins. *Power Electronics, 3rd rev edition*. John Wiley & Sons, New York, 2002.

[16] Wikipedia contributors. Skin effect [Internet]. Wikipedia, The Free Encyclopedia; 2013 May 21, 15:08 UTC [cited 2013 May 24]. Available from: http://en.wikipedia.org/w/index.php?title=Skin_effect&oldid=556115078.

[17] F.E. Terman. *Radio Engineers' Handbook*. McGraw-Hill, 1943.

[18] Electrical Engineering. [Online] [cited 2013 May 15]. Available from: http://www.electrical4u.com/hysteresis-eddy-current-iron-or-core-losses-and-copper-loss-in-transformer

[19] E-mail from Kenneth Lind, Trafikverket (2013 February 20).

[20] Trafikverket (2013 February 11) *Sveriges vägnät* [Online] [cited 2013 June 5]. Available from: http://www.trafikverket.se/Privat/Vagar-och-jarnvagar/Sveriges-vagnat/

[21] OLEV Technologies (2013) *Background* [Online] [cited 2013 May 12]. Available from: http://olevtech.com/about-us/fact-sheet/

[22] OLEV Technologies (2012 August) *Magnetic Field Design for Low EMF and High Efficiency Wireless Power Transfer System in On-Line Electric Vehicles* [Online] [cited 2013 May 12] Available from: http://olevtech.com/wp-content/uploads/2012/08/CIRP-Design-2011-Paper35.pdf

[23] OLEV Technologies (2012 August) [Online] [cited 2013 May 12]. Available from: http://olevtech.com/wp-content/uploads/2012/08/OLEV_Product_Sheet_Long.pdf

[24] PRIMOVE (2013) *The technology behind primove* [Online] [cited 2013 May 12]. Available from: http://primove.bombardier.com/about/technical-principle

[25] PRIMOVE (2013) *PRIMOVE automotive* [Online] [cited 2013 June 5]. Available from: http://primove.bombardier.com/application/automotive/

[26] Wikipedia contributors. Supermalloy [Internet]. Wikipedia, The Free Encyclopedia; 2013 Apr 19, 21:25 UTC [cited 2013 May 29]. Available from:

http://en.wikipedia.org/w/index.php?title=Supermalloy&oldid=551192006.

[27] Magnetic Metals (2013) *Characteristics of Core Materials – Supermalloy* [Online] [cited 2013 May 19]. Available from: http://www.magmet.com/tapewound/supermalloy.php

[28] E. Bellone. *A World on Paper: Studies on the Second Scientific Revolution*. Cambridge: MIT Press, 1980.

[29] R.A. Serway. *Physics for Scientists and Engineers with Modern Physics, 4th edition*. Prentice Hall, New Jersey, 1996, p, 687.

[30] Wikipedia contributors. Vacuum permittivity [Internet]. Wikipedia, The Free Encyclopedia; 2013 May 17, 15:06 UTC [cited 2013 April 2]. Available from: http://en.wikipedia.org/w/index.php?title=Vacuum_permittivity&oldid=555522759.

[31] I.S. Grant, W.R. Phillips. *Electromagnetism, 2nd edition*. Manchester Physics, 2008.

[32] Wikipedia contributors. Gauss's law for magnetism [Internet]. Wikipedia, The Free Encyclopedia; 2013 May 9, 19:37 UTC [cited 2013 April 2]. Available from: http://en.wikipedia.org/w/index.php?title=Gauss%27s_law_for_magnetism&oldid=554334849.

[33] F. Ulaby. *Fundaments of applied electromagnetics, 5th edition*. Prentice Hall, New Jersey, 2007, p. 255.

[34] C.R. Nave (1999) *Magnetic* flux [Online] [cited 2013 April 3]. Available from: http://hyperphysics.phy-astr.gsu.edu/hbase/magnetic/fluxmg.html

[35] C.R. Nave. (1998) *Faraday's Law* [Online] [cited 2013 April 5]. Available from: http://hyperphysics.phy-astr.gsu.edu/hbase/electric/farlaw.html

[36] R.F. Harrington. *Introduction to electromagnetic engineering*. Dover Publications, Mineola, 2003, p.56.

[37] C.R. Nave. (1999) *Maxwell's equations* [Online] [cited 2013 April 5]. Available from: http://hyperphysics.phy-astr.gsu.edu/hbase/electric/maxeq.html

[38] Wikipedia contributors. Vacuum permeability [Internet]. Wikipedia, The Free Encyclopedia; 2013 Mar 1, 05:08 UTC [cited 2013 April 4]. Available from: http://en.wikipedia.org/w/index.php?title=Vacuum_permeability&oldid=541430423.

[39] C.R. Nave. (1999) *Inductance of a Coil* [Online] [cited 2013 April 6]. Available from: http://hyperphysics.phy-astr.gsu.edu/hbase/magnetic/indcur.html

[40] MIT [Online] [cited 2013 April 8]. Available from: http://web.mit.edu/viz/EM/visualizations/notes/modules/guide11.pdf

[41] E. Waffenschmidt. *Coupling Factor* [Online] [cited 2013 April 8]. Available from: http://www.wirelesspowerconsortium.com/technology/coupling-factor.html

[42] D.C. Giancoli. *Physics: principles with applications, 5th edition*. Pretence Hall, New Jersey, 1998, p. 624.

[43] Wikipedia contributors. Frequency changer [Internet]. Wikipedia, The Free Encyclopedia; 2013 Apr 27, 15:23 UTC [cited 2013 April 8]. Available from: http://en.wikipedia.org/w/index.php?title=Frequency_changer&oldid=552427459.

[44] M.Y. Lee, "Three-level Neutral-point-clamped Matrix Converter Topology," Ph.D. dissertation, University of Nottingham, 2009.

[45] B.W. Williams. "Chapter 11," *Power electronics: devices and applications, 2nd edition*. Macmillan, Basingstoke, 1992.

[46] M. Stutz. (1999) *Rectifier circuits* [Online] [cited 2013 May 20]. Available from: http://www.allaboutcircuits.com/vol_3/chpt_3/4.html

[47] J. Miniböck, J.W. Kolar. *A Novel 10 kW Three-Phase High Power Density (2-U) Telecommunications Unity Power Factor Rectifier Module* [Online] [cited 2013 May 20]. Available from: http://www.pes.ee.ethz.ch/uploads/tx_ethpublications/miniboeck_CIPS02.pdf

[48] M. Alaküla, P. Karlsson. "AC Inverters," *Power Electronics*. p. 28.

[49] Power-One (2013) *Efficient Power Solutions* [Online] [cited 2013 May 20]. Available from: http://www.power-one.com/renewable-energy/efficient-power-solutions

10 Appendix

10.1 Classic electrodynamics

The fundamental laws of electromagnetism which explains the magnetic coupling between the primary and secondary side of the inductive energy transfer system is here explained in more detail.

10.1.1 Maxwell's equations

The four corner stones of electromagnetism, and therefore wireless power transfer, are Maxwell's equations, consisting of Gauss's law for electric field, Gauss's law for magnetic field, the Maxwell-Faraday equation and Ampere's circuit law. What these equations mean is that if a current is run through a conductor, a magnetic field is induced. If this magnetic field varies in time and/or space, an electric field is induced, and if another conductor is subjected by this electric field, its electrons are moved by this field due to Lorentz force. This movement of electrons means that a current is now running through the second conductor, with its source being the first contact with which it has no galvanic contact.

10.1.1.1 Gauss's law for electric field

Formulated by Carl Friedrich Gauss in 1835[28] the law for electric field states the following:

"The net outward normal electric flux through any closed surface is proportional to the total electric charge enclosed within that closed surface." [29]

As an equation this can be written as:

$$\oiint_S \mathrm{E} \cdot \mathrm{dA} = \frac{Q}{\epsilon_0} = \phi_E \qquad (52)$$

where *E* is the electric field, *dA* is an infinitesimal element of the enclosed area *S* (see Figure 33), *Q* is the total electric charge within the enclosed area, ϵ_0 is the electric constant, also known as vacuum permittivity (approximately equal to $8.854 \cdot 10^{-12}$ F·m^{-1} [30]) and ϕ_E is the electric flux[31].

[28] E. Bellone. *A World on Paper: Studies on the Second Scientific Revolution*.
[29] R.A. Serway. *Physics for Scientists and Engineers with Modern Physics, 4th edition*, p, 687.
[30] Wikipedia (2013) Vacuum permittivity.
[31] I.S. Grant, W.R. Phillips. *Electromagnetism, 2nd edition*. Manchester Physics.

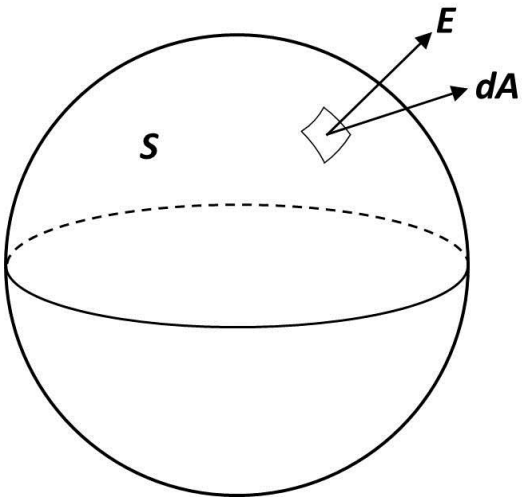

Figure 33: Graphical explanation of the parameters in equation (52).

10.1.1.2 Gauss's law for magnetism

Gauss also formulated a law for magnetism which is similar to his law for electric fields, and the equation can be written as:

$$\oiint_S \mathrm{B} \cdot \mathrm{dA} = 0 \qquad (53)$$

where *B* is the magnetic field[32] (see Figure 34). What this equation means is that through any enclosed surface, the number of magnetic field lines entering the volume the surface holds, equals the number of field lines exiting. This can be demonstrated with a permanent magnet, whose south pole and north pole are equally strong

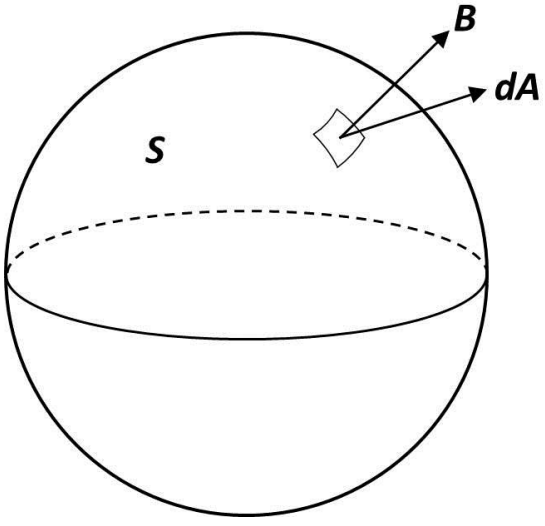

Figure 34: Graphical explanation of the parameters in equation (53).

[32] Wikipedia (2013) Gauss's law for magnetism.

10.1.1.3 Faraday's law of induction and Maxwell-Faraday equation

Michael Faraday discovered electromagnetic induction in 1831[33], and his law says that in an electric circuit, an electromotive force, emf (denoted ε), is induced by the time rate of change of the magnetic flux through the circuit. The magnitude of the magnetic flux depends on the strength of the magnetic field and the size of the open surface through which the field lines passes. The equation for this can be written as:

$$\Phi_B = \iint_S \mathrm{B} \cdot \mathrm{dA} \qquad (54)$$

where Φ_B is the magnetic flux[34]. As stated previously by the law, the emf comes from the time rate of change of the magnetic flux, which can be written as:

$$\varepsilon = -\frac{d\Phi_B}{dt} \qquad (55)$$

If the flux passes through a coil with more than one turn, the equation can be extended to the following:

$$\varepsilon = -N \cdot \frac{d\Phi_B}{dt} \qquad (56)$$

where *N* is the number of turns, and Φ_B is the magnetic flux through a single loop[35].

However Faraday's law of induction is not one of Maxwell's four equations directly as it is written. Instead the Maxwell-Faradays equation is used, which is a generalisation of the previously mentioned law. The Maxwell-Faraday equation states that there is always an electric field accompanied by a time-varying magnetic field. The equation can be written as:

$$\oint_{\delta\Sigma} \mathrm{E} \cdot dl = -\int_{\Sigma} \frac{\delta \mathrm{B}}{dt} \cdot d\mathrm{A} \qquad (57)$$

where *Σ* is a surface limited by the closed contour *δΣ* and *dl* is and infinitesimal vector element of the contour *δΣ* [36]. The right side is the same as in equation (55).

10.1.1.4 Ampère's circuit law

Discovered by André-Marie Ampère, Ampère's circuit law correlates the integrated magnetic field around a closed loop to the current passing through it. The original law can only be used to determine the magnetic field around a closed loop with a known current, and vice versa, in the case of static electric field, meaning magnetostatic situations[37]. This law has then been expanded to the Maxwell-Ampère equation, as can be written as:

$$\oint_C \mathrm{B} \cdot dl = \iint_S \left(\mu_0 \mathrm{J} + \mu_0 \varepsilon_0 \frac{\delta}{\delta t} \mathrm{E}\right) \cdot \mathrm{dS} \qquad (58)$$

[33] F. Ulaby. *Fundaments of applied electromagnetics, 5th edition*, p. 255.
[34] C.R. Nave (1999) *Magnetic* flux
[35] C.R. Nave. (1998) *Faraday's Law* [Online].
[36] R.F. Harrington. *Introduction to electromagnetic engineering*.
[37] C.R. Nave. (1999) *Maxwell's equations* [Online].

where *S* is a surface limited by the closed contour *C*, *J* is the current density through *S* and μ_0 is the magnetic constant or the vacuum permeability (equals $4\pi \cdot 10^{-7}$ $H \cdot m^{-1}$ [38]). The right side of this equation can be rewritten resulting in the following equation

$$\oint_C \mathrm{B} \cdot dl = \mu_0 \cdot \left(\mathrm{I} + \varepsilon_0 \frac{d\Phi_E}{dt} \right) \quad (59)$$

where *I* is the current through the surface.

10.1.2 Inductance and mutual inductance

As stated in equation (54), the magnetic flux through a surface depends on both the size of the surface and the magnetic field. The magnetic field comes from running a current through a closed loop, as shown in equation (58), meaning that doing so generates a magnetic flux with the closed loop as the source. It then becomes clear that there is a relationship between the current through the loop and the generated magnetic flux. This relationship is linear and the proportionality coefficient is called inductance, or self-inductance (denoted *L*).

$$\Phi = L \cdot I \quad (60)$$

Although this equation shows that the inductance can be calculated as the ratio between the magnetic flux and the current, it can also be shown that the inductance does not depend on the flux or current, but rather exclusively depends on geometrical factors and physical properties.

$$L = \frac{\mu_0 \mu_r N^2 A}{l} \quad (61)$$

where μ_r is the relative permeability of the material, *N* is the number of turns in the coil, *A* is the cross sectional area and *l* is the length of the coil[39].

As equation (53) shows, the magnetic field in and out of a surface enclosing a volume always equals zero. However the magnetic field can still interact with other object on its way back into the volume. If for example a second loop is placed near the first, part of the magnetic flux from the original passes through the second, as a result of magnetic field from the first, denoted B_1. Provided the area of the second loop is known, the flux from the first loop going through the second can be calculated. This part of the magnetic flux is called mutual flux, denoted Φ_{12} and is calculated as shown below:

$$\Phi_{12} = \int_{S_2} B_1 \cdot dS_2 \quad (62)$$

The same is true if the current is instead run through the second loop and the first receives part of the total magnetic flux generated by the current, and equation (62) is rewritten to:

$$\Phi_{21} = \int_{S_1} B_2 \cdot dS_1 \quad (63)$$

Just as there is a relationship between the current through a loop and the magnetic flux it generates, the same applies with the current through a loop and the magnetic flux from it that a second loop

[38] Wikipedia (2013) Vacuum permeability.
[39] C.R. Nave. (1999) *Inductance of a Coil*.

experiences. This relationship is for the sake of simplicity assumed to also be linear and it is called mutual inductance, denoted *M*. For the two previous cases this can be written as:

$$\Phi_{12} = M_{12} \cdot I_1 \quad (64)$$

$$\Phi_{21} = M_{21} \cdot I_2 \quad (65)$$

Using the reciprocity theorem it can then be shown that M_{12} equals M_{21} and can therefore be written as only M [40].

$$M_{12} = M_{21} \equiv M \quad (66)$$

10.1.3 Flux linkage of coils

A coil is simply several loops of conductors stacked on top of each other forming a cylinder of loops, or a conductor turned several times. The reason to wound several turns is that each turn generates a magnetic flux, and total magnetic flux from the coil becomes the sum of all the individual turns. This total magnetic flux is called flux linkage and is denoted Ψ.

$$\Psi = N \cdot \Phi \quad (67)$$

As seen in equation (61), the inductance depends on the number of turns, and by combining equations (60) and (67) the inductance of a coil can be calculated using the current through each turn and the flux linkage.

$$L = \frac{\Psi}{I} \quad (68)$$

The same can be done with the mutual inductance between two coils where the magnetic field, which passes through the second coil, increases with each turn. The mutual flux interacts with each turn in the coil and the flux linkage becomes the product of the number of turns and the mutual flux for one turn.

$$\Psi_{12} = N_2 \Phi_{12} \quad (69)$$

The mutual inductance between the two coils is then calculated as:

$$M = \frac{\Psi_{12}}{I_1} \quad (70)$$

Since the mutual inductance is proportional to N_2 and the flux linkage is proportional to N_1, it becomes clear that the mutual inductance is proportional to both N_1 and N_2.

$$M \propto N_1 N_2 \quad (71)$$

Equation (61) shows that the inductance of a coil is specified by the geometrical shape and physical properties of the conductor, and by the permeability of the medium inside the coil. In the case of the mutual inductance between the two coils, it is also dependent on the distance and relative position of the coils. The mutual inductance is proportional to the square root of the product of the two coils' self-inductances, and the proportionality constant is called the coupling factor and is denoted *k*.

[40] MIT.

$$M = k \cdot \sqrt{L_1 L_2} \quad (72)$$

$$0 \leq k \leq 1 \quad (73)$$

The coupling factor evaluates the magnetic coupling between the coils and only depends on the relative position between the two coils and the physical properties of the media between them and the media of the cores. If *k* equals 1, the magnetic coupling is perfect and all the generated flux passes through the receiving coil whereas if *k* is 0, the two coils are independent of each other[41].

10.1.4 Electromotive force

As shown with equation (55) Faraday's law states that the time rate of change of magnetic flux through a loop or a coil induces an electromotive force, emf. Contradictory to what the name suggests, the emf is not a force measured in newton [N], but an electrical potential (voltage) measured in volts. If the coil is connected to a circuit and this circuit is closed, the induced voltage causes a current to start running through the entire circuit. According to Lenz's law this current will in turn generate a magnetic field which tends to oppose the change in magnetic flux, which induced the current in the first place[42]. This leads to the two coils repelling each other, just like two permanent magnets would if their north poles (or south poles) would face each other.

10.2 Power electronics

This section further explains the necessary components between the power grid and the magnetised transformer half in the road.

10.2.1 Frequency changer

Because of the previously stated need for a high frequency to achieve a feasible power transfer, the frequency from the source (power grid or generator) must be changed. Unlike with the case of transforming one voltage level to another, changing to frequency is a significantly harder task and also more expensive.

A frequency changer is an AC/AC converter which utilises the option to change the frequency while transforming from DC to AC and back again. First the AC from the source is rectified and then using a power inverter it is changed back into AC again but when this is done a new frequency can be chosen. If another level of the voltage is also required, a transformer can be added to either the in- or output AC circuitry. An additional gain with this is that the transformer serves as a galvanic isolation between the in- and output circuits[43].

AC/AC converters can be categorized into four groups:

- AC-DC-AC converters
- Cycloconverters
- Hybrid matrix converters
- Matrix converters

The AC-DC-AC converter exists for both voltage sources (voltage-source inverter converter) and current sources (current-source inverter converter). The rectifier part of these consists of a phase-

[41] E. Waffenschmidt. *Coupling Factor*.
[42] D.C. Giancoli. *Physics: principles with applications, 5th edition*, p. 624.
[43] Wikipedia (2013) Frequency changer.

controlled switching bridge, the DC link consists of a series inductor on one of both DC connectors (CSI converter), or a capacitance in parallel (VSI converter) and the inverter consists of three transistor half-bridges[44], see Figure 35.

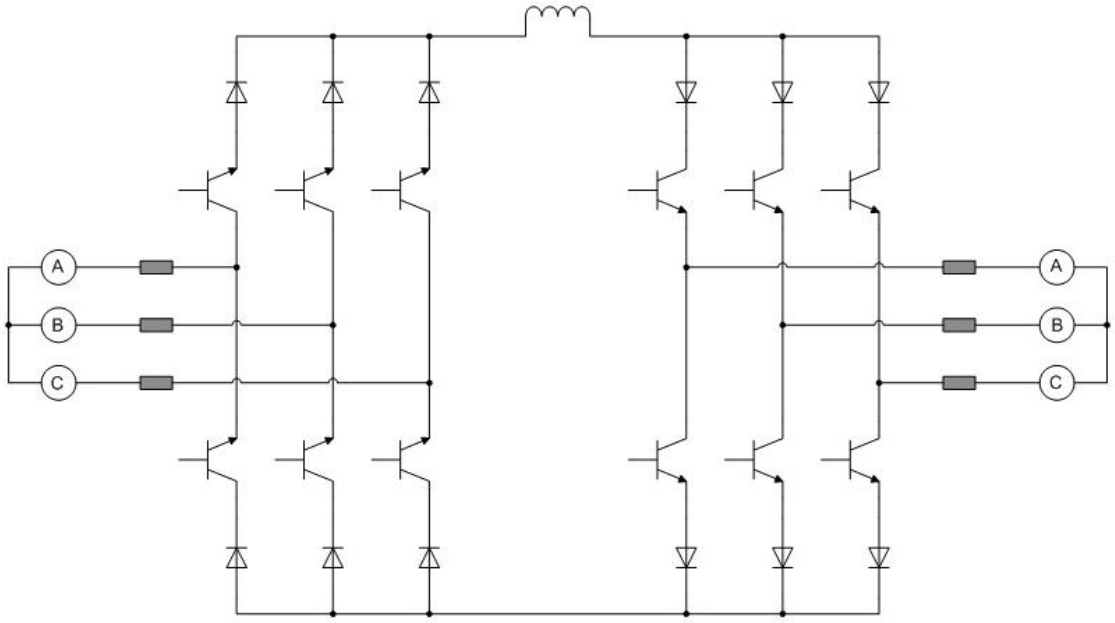

Figure 35: A three-phase source connected to a rectifier in the form of a phase-controlled switching bridge, an inductor as the DC link and three transistor half-bridges connected to a three-phase load.

10.2.2 Rectifier

The simplest way to rectify an alternating current is to use a single diode in its path which only lets the current pass on either the positive or the negative half-wave, called half-wave rectifier. This solution is not very effective since only half of the wave gets used, and the DC voltage becomes the peak value divided by π.

The problem with only using the power half of the time is solved by constructing a full-wave bridge of diodes, see Figure 36. This configuration converts the full wave into one polarity; either positive or negative, meaning the dc voltage becomes twice that of a half-wave rectifier[45].

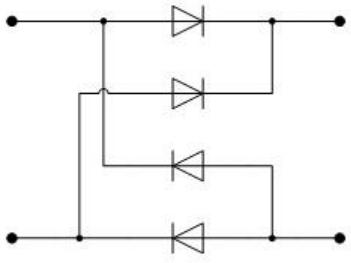

Figure 36: Full-wave bridge rectifier for one phase.

Of course for most high power application three-phase is needed, which is just as accomplishable as for one phase (both half- and full-wave). The difference is that thyristors are normally used instead of diodes since this allows the output voltage to be regulated. The rectifier is constructed of six diodes

[44] M.Y. Lee, "Three-level Neutral-point-clamped Matrix Converter Topology," Ph.D. dissertation.
[45] B.W. Williams. "Chapter 11," *Power electronics: devices and applications, 2nd edition*.

(or thyristors) as seen in Figure 37. Because of the 6 diode configuration, the rectifiers are often called six-pulse rectifier. For these the DC-voltage becomes

$$\frac{3\sqrt{3}V_{peak}}{\pi} \quad (74)$$

for diodes, and

$$\frac{3\sqrt{3}V_{peak}}{\pi}\cos\alpha \quad (75)$$

for thyristors, where α is the firing angle (the phase angle of the voltage at which it starts conducting) of the thyristor. Although the DC-voltage for the thyristor option is smaller, the advantage is that is rectifier can be controlled, since it is possible to determine when a thyristor should conduct.

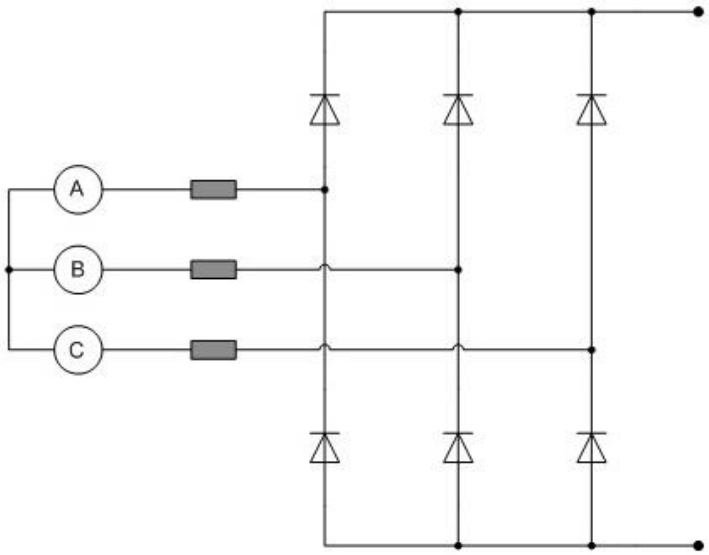

Figure 37: Three-phase diode rectifier.

While the three-phase, full-wave rectifier is better than single-phase equivalences and the three-phase, half-wave rectifier, it is not without problems. The six-pulse rectifiers produce a significant amount of harmonic distortions on both the DC- and AC-connections. To solve this problem, two six-pulse bridges can be series connected into a twelve-pulse bridge. These works so that the source is connected to the rectifier through one Y-Y and one Y-Δ connection, see Figure 38. The second connection leads to a shift of 30° between the two rectified signals, and when the two six-pulse bridges are series connected the result is 12 DC-pulses per period instead of 6[46], se Figure 39.

[46] M. Stutz. (1999) *Rectifier circuits*.

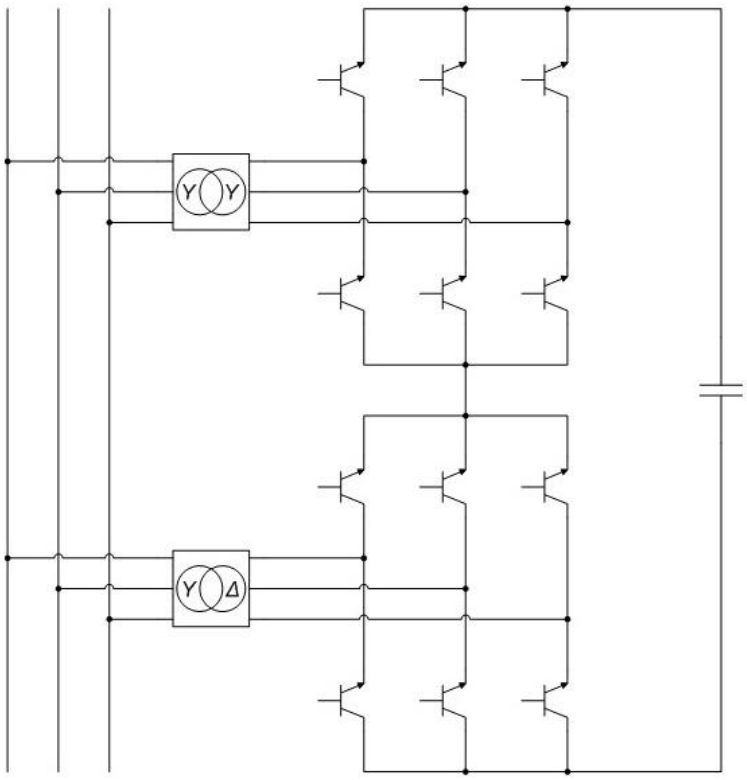

Figure 38: Twelve-pulse rectifier.

For a 12-pulse converter the DC-voltage becomes:

$$\frac{6\sqrt{3}V_{peak}}{\pi}\cos\alpha \qquad \textbf{(76)}$$

A well-constructed rectifier has an efficiency of 95 % or more[47].

[47] J. Miniböck, J.W. Kolar. *A Novel 10 kW Three-Phase High Power Density (2-U) Telecommunications Unity Power Factor Rectifier Module*

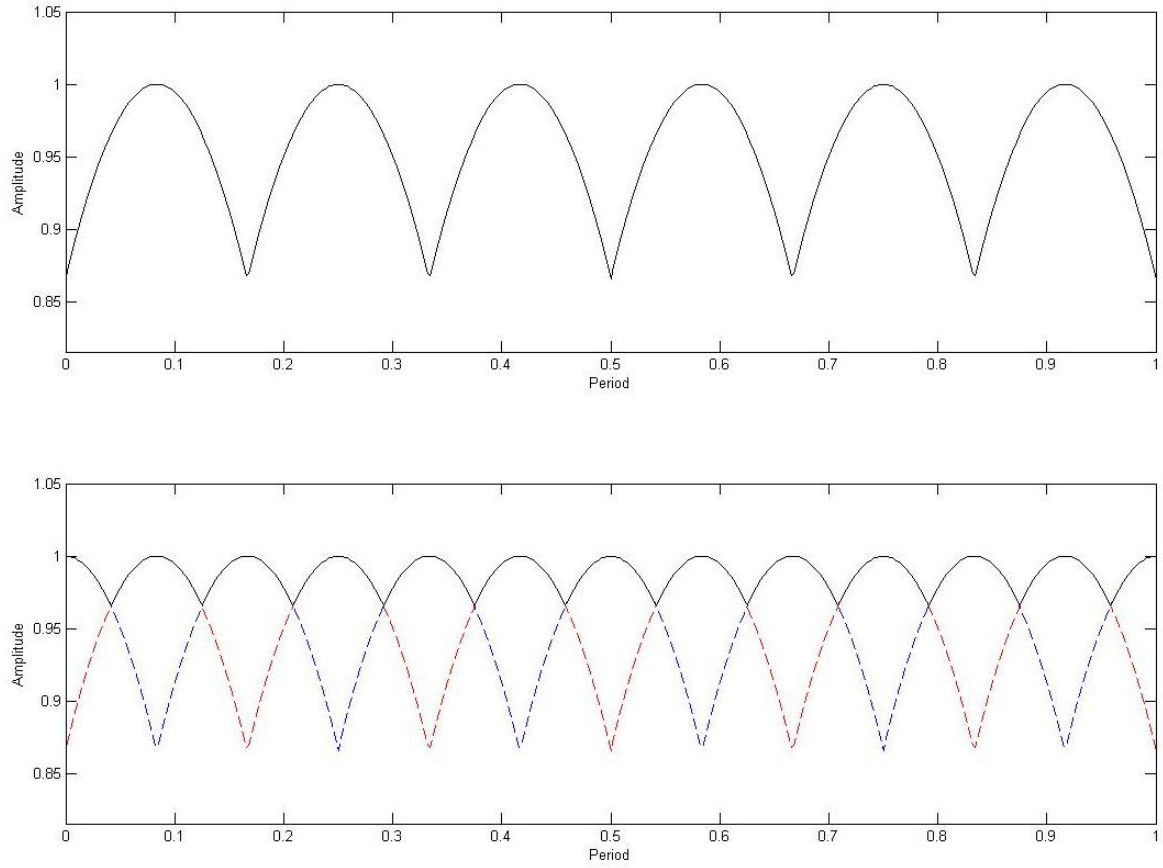

Figure 39: In the upper figure the DC-pulses from a six-pulse rectifier are shown, and in the one below is the equivalent of the 12-pulse rectifier, with the Y-Y (red) and the Y-Δ (blue) connections shown as dashed lines.

10.2.3 Power inverter

The next part of the frequency changer is to transform the DC into an AC with the new desired frequency and voltage level, which is done with a DC-AC or power inverter. This is achieved by connecting the DC-lines to three transistor half-bridges (with a snubber for each transistor) with each output terminal connected to one of the phase connectors of the load[48], see Figure 40.

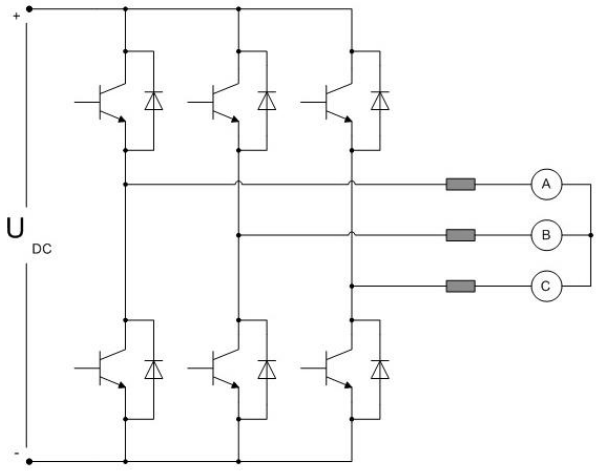

Figure 40: Power inverter constructed with three transistor half-bridges, connected to a three-phase load.

[48] M. Alaküla, P. Karlsson. "AC Inverters," *Power Electronics*. p. 28.

Each transistor is controlled through a control signal which determines whether the transistor should conduct or block, and for how long. With this method, the phase shift between each phase connected to the load can be controlled as well and therefore achieve a three phase system with a new frequency more suited for the application than the 50 Hz grid. A power inverter has an efficiency of about 90-95 %[49].

10.2.4 Complex power

Because some of the magnetic flux only links with the coil itself, this energy causes the current through the coil to lag compared to the voltage producing the current. Regardless of the phase shift between the time-varying voltage and current, the power is calculated as

$$p(t) = u(t) \cdot i(t) \quad (77)$$

Because of the lag, the maximum value of the power is not equal the maximum value of the voltage times that of the current. Instead, this multiplication is called complex power, is denoted *S* and has the unit volt-ampere [VA]. The complex power consists of two parts, the real part, active power [W], and the imaginary part, reactive power [VAr], see Figure 41.

$$S = P + jQ \quad (78)$$

The phase shift between the voltage and current is denoted φ and the cosine of this value is the relative active power, whereas the sine is the relative reactive power. These relative powers are multiplied with what is called apparent power ($|S|$), which is the magnitude of the complex power to get the value of the active and reactive power respectively.

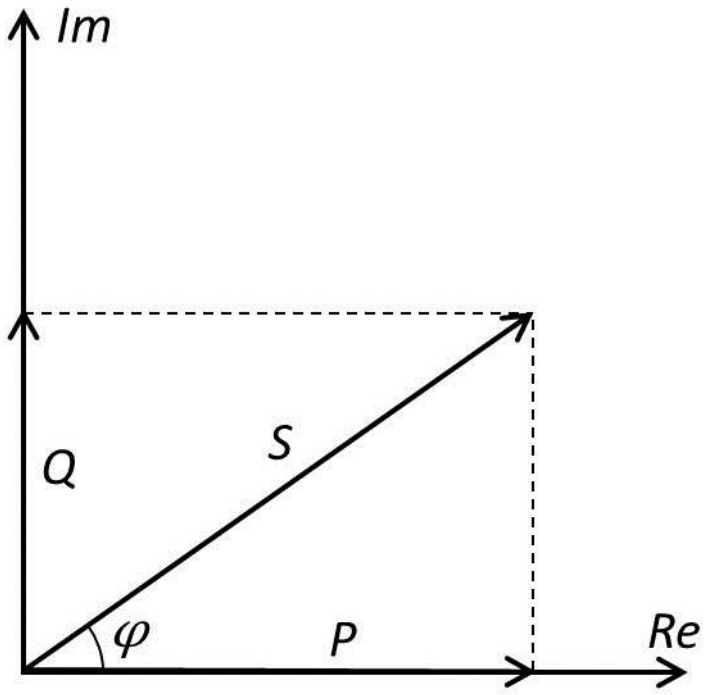

Figure 41: Vector representation of complex power and its components.

A final important term for complex power is the power factor and is used to determine how efficient or well rated a power distribution system is

[49] Power-One (2013) *Efficient Power Solutions*.

$$PF = \cos\varphi \quad (79)$$

A lower power factor is caused by a higher inductance or capacitance in the circuit since this increase the reactive power component, and therefore the phase shift angle. This means that the circuit has more circulating current due to energy that returns to the source from the energy storage in the load. These currents lead to higher losses in and therefore a lower efficiency. When voltage and current are in phase the power factor is in unity meaning the system only draws active power from the source.

10.3 Three-phase transformer matrix

Component description of equation (19) for a three-phase transformer.

$$\begin{pmatrix} U_1 \\ U_2 \\ U_3 \\ 0 \\ 0 \\ 0 \end{pmatrix} = \left(\begin{pmatrix} R_1 + j\omega M_{11} & j\omega M_{12} & j\omega M_{13} & j\omega M_{14} & j\omega M_{15} & j\omega M_{16} \\ j\omega M_{21} & R_2 + j\omega M_{22} & j\omega M_{23} & j\omega M_{24} & j\omega M_{25} & j\omega M_{26} \\ j\omega M_{31} & j\omega M_{32} & R_3 + j\omega M_{33} & j\omega M_{34} & j\omega M_{35} & j\omega M_{36} \\ j\omega M_{41} & j\omega M_{42} & j\omega M_{43} & R_4 + j\omega M_{44} & j\omega M_{45} & j\omega M_{46} \\ j\omega M_{51} & j\omega M_{52} & j\omega M_{53} & j\omega M_{54} & R_5 + j\omega M_{55} & j\omega M_{56} \\ j\omega M_{61} & j\omega M_{62} & j\omega M_{63} & j\omega M_{64} & j\omega M_{65} & R_6 + j\omega M_{66} \end{pmatrix} + \begin{pmatrix} 0 & 0 & 0 & 0 & 0 & 0 \\ 0 & 0 & 0 & 0 & 0 & 0 \\ 0 & 0 & 0 & 0 & 0 & 0 \\ 0 & 0 & 0 & R_{load} & 0 & 0 \\ 0 & 0 & 0 & 0 & R_{load} & 0 \\ 0 & 0 & 0 & 0 & 0 & R_{load} \end{pmatrix} \right) \begin{pmatrix} I_1 \\ I_2 \\ I_3 \\ -I_4 \\ -I_5 \\ -I_6 \end{pmatrix}$$

10.4 AC-resistance due to proximity effect

$$R_{AC} = R_{DC}\left(Re(M) + \frac{(m^2-1)Re(D)}{3}\right)$$

$$M = \alpha h \coth(\alpha h)$$

$$D = 2\alpha h \tanh\left(\frac{\alpha h}{2}\right)$$

$$\alpha = \sqrt{\frac{j\omega\mu_0\eta}{\rho}}$$

$$\eta = N_1\frac{a}{b}$$

where N_1 is the number of turns per layer, a is the width of the (square) conductor, b is the width of the winding window and h is the height of the (square) conductor. Note that this equation can be applied approximately to round conductor by calculate it as a square conductor with the same cross sectional area.